In Vivo and *In Vitro* Characterization of Miconazole Nitrate Loaded Transethosomes for the Treatment of Cutaneous Candidiasis

M.Phil Thesis

by

MARYAM RASOOL

Department of Pharmacy
Faculty of Biological Sciences
Quaid-i-Azam University
Islamabad, Pakistan
2022

In Vivo and *In Vitro* Characterization of Miconazole Nitrate Loaded Transethosomes for the Treatment of Cutaneous Candidiasis

Thesis Submitted by

MARYAM RASOOL

Registration No. 02332013006

to

Department of Pharmacy,

In Partial Fulfillment of Requirements for the Degree of

Master of Philosophy

in

Pharmacy (Pharmaceutics)

Department of Pharmacy
Faculty of Biological Sciences
Quaid-i-Azam University
Islamabad, Pakistan

2022

AUTHOR'S DECLARATION

I, Maryam Rasool, hereby state that my M.Phil. Thesis titled **"*In Vivo* and *In Vitro* Characterization of Miconazole Nitrate Loaded Transethosomes for the Treatment of Cutaneous Candidiasis"** submitted to the Department of Pharmacy, Faculty of Biological Sciences, Quaid-i-Azam University Islamabad, Pakistan for the award of degree of Master of Philosophy in Pharmacy (Pharmaceutics) is the result of research work carried out by me. I further declare that the results presented in this thesis have not been submitted for the award of any other degree from this university or anywhereelse in the country/world and the University has right to withdraw my M. Phil degree, if my statement is found incorrect anytime even after my graduation.

_____

MARYAM RASOOL

DATE: _____

PLAGIARISM UNDERTAKING

I, Maryam Rasool, solemnly declare that research work presented in this thesis titled "***In Vivo* and *In Vitro* Characterization of Miconazole Nitrate Loaded Transethosomes for the Treatment of Cutaneous Candidiasis**" is solely my research work with no significant contribution from any other person. Small contribution/help wherever taken have been duly acknowledged and that complete thesis has been written by me.

I understand zero tolerance policy of Quaid-i-Azam University, Islamabad, and HEC towards plagiarism. Therefore, I, as an author of the above titled dissertation, declare that no portion of my thesis is plagiarized, and every material used as reference is properly referred/cited.

I undertake that if I am found guilty of committing any formal plagiarism in the above titled thesis even after award of M. Phil degree the university reserves the right to withdraw or revoke my M. Phil degree and that HEC and University has the right to publish my name on the HEC/University Website on which names of those students are placed who submitted plagiarized thesis.

_____

MARYAM RASOOL

APPROVAL CERTIFICATE

This is certified that the dissertation titled "***In Vivo* and *In Vitro* Characterization of Miconazole Nitrate Loaded Transethosomes for the Treatment of Cutaneous Candidiasis**" submitted by **Miss. Maryam Rasool**, to the Department ofPharmacy, Faculty of Biological Sciences, Quaid-i-Azam University Islamabad, Pakistan is accepted in its present form as it is satisfying the dissertation requirements for the degree of Master of Philosophy in **Pharmacy (Pharmaceutics).**

Supervisor

Dr. Hussain Ali
Associate Professor
Department of Pharmacy,
Quaid-i-Azam University
Islamabad, Pakistan

External Examiner

(Name)
Designation
Department of Pharmacy,
Quaid-i-Azam University
Islamabad, Pakistan

Chairman

Prof. Dr. Ihsan-Ul-Haq
Chairman
Department of Pharmacy,
Quaid-i-Azam University
Islamabad, Pakistan

Dated _____

DEDICATION

First of all, I would like to thank AlmightyALLAH for everything in my life. Without His guidance I would never be able to accomplish anything in my whole life

&

To my mother and father,
I could never have done this without your faith,
support, and constant encouragement.
Thank you for teaching me to believe in myself, ALLAH, and in my dreams, alongwith all hardworking and respected teachers.

TABLE OF CONTENTS

Acknowledgement

In the name of Allah (S.W.T), the most gracious, the most merciful and the only one because of whom I stand where I am today. No word of praise is good enough nor is any amount of gratitude sufficient to thank Him for blessing us with everything. Firstly, I gratefully acknowledge my research supervisor, **Dr. Hussain Ali** for his supervision, support, advice, and guidance from the very early stage of this research. Without his overwhelming encouragement, careful supervision, and kind suggestionsI would not be able to accomplish this work. I profusely thank to all the faculty members of department of pharmacy, QAU for providing and maintaining learning opportunities for every student. I would like to extend my heartfelt thanks to my **parents** and family specially my parents who means the whole world to me. No words can express my gratitude, respect, and love for my beloved parents. I cannot even take a single footstep without their prayers, help, motivation, and support. They always stand by me during the ups and downs of mylife. I am honoured to have such a loving and caring family. I would also like to thank my best friend **Sidra Bashir** for your help and support throughout my research project.

MARYAM RASOOL

List of Tables

List of Figures

List of Abbreviations

Abbreviation	Description
Conc.	Concentration
Cn	Concentration of drug released in medium at sample
Ci	Concentration in acceptor medium at sample ith time
DLS	Dynamic light scattering
DSC	Differential scanning calorimetry
EE	Entrapment efficiency
ER	Enhancement ratio
FTIR	Fourier transform infrared spectroscopy
Jss	Steady state flux
Kp	Permeability coefficient Kp
MCZN	Miconazole Nitrate
MCZN TESs	Miconazole Nitrate transethosomes
MCZN TESs Gel	Miconazole Nitrate loaded transethsomal gel
n	Diffusion exponent for drug release
PL90G	Phospholipon 90 G
PDII	Primary dermal irritancy index
PDI	Polydispersity index
PS	Particle Size
PBS	Phosphate buffer saline
S 80	Span 80
SDA	Sabouraud dextrose agar
TESs	Transethosomes

UV	Ultraviolet-Visible
UDV	Ultra-deformable vesicles
Vr	Volume of acceptor medium
Vs	Volume of sample withdrawn from the medium
ZOI	Zone of inhibition
ZP	Zeta potential

Abstract

In case of cutaneous candidiasis topical delivery is preferable because of easy application and targeted treatment on the site of infection. Miconazole Nitrate (MCZN) is a broad-spectrum antifungal drug that possesses dual mechanism of action making it superior to other azoles. Also, it has rare innate and cross resistance with other azoles. However, it has very poor skin penetration. So, its conventional topical formulations are not efficient enough to treat deep seated fungal infections. To overcome this problem Miconazole Nitrate loaded transethosomes (MCZN TESs) and chitosan-based Miconazole Nitrate loaded transethosomes gel was formulated (MCZN TESs Gel). The thin film hydration method was employed for formulation of MCZN TESs, and Box-Behnken Design was used for its optimization. Lipid, surfactant, and drug were selected as independent variable and particle size (PS), zeta potential (ZP). Polydispersity index (PDI) and entrapment efficiency (EE) were selected as dependent variables. PS, ZP, PDI and EE were investigated for optimized formulation and FTIR analysis was carried out to check any interaction between drug and its excipients and DSC analysis was also performed. Deformability and elasticity of optimized formulation were also analysed. TESs were incorporated in chitosan gel and MCZN TESs Gel was characterized in terms of physical appearance, homogeneity, pH, spreadability and rheological properties. *In vitro* and ex vivo permeation and skin deposition studies were also performed to check drug release and its penetration and deposition within skin layers respectively. Skin irritation studies were performed. *In vitro* antifungal assay was carried out to check enhanced antifungal potential of developed MCZN TESs Gel in comparison to Marketed Gel. *In vivo* antifungal studies were also investigated. Optimized formulation had the PS of 224.8 ± 5.1 nm, ZP 21.1 ± 1.10 mV, PDI 0.207 ± 0.009 and EE 93.12 ± 0.101%. FTIR results showed no interaction and DSC results showed enhanced solubility of drug in final formulation. DI was 0.94 and %DI was 94.196%. elasticity was 2.11 ± 0.02, proving that optimized formulation of MCZN TESs was deformable as well as elastic. Moreover, MCZN TESs Gel was uniform with desirable pH, spreadability and viscosity. *In vitro* release of MCZN TESs and MCZN TEs Gel showed prolong release behaviour in comparison to drug dispersion. MCZN TESs and MCZN TESs Gel had enhanced penetration and deposition in comparison to drug gel (MCZN Gel) and Marketed Gel. Skin irritation studies showed gel was non-irritant and safe. *In vitro* antifungal assay and *in vivo* studies showed superiority of

MCZN TESs Gel in comparison with MCZN Gel and Marketed Gel. From studies it was clear that MCZN TESs were successfully optimized and characterized with enhanced penetration and antifungal properties for the treatment of cutaneous candidiasis.

CHAPTER 1

INTRODUCTION

1. INTRODUCTION

1.1. Background

Fungal infections of skin and nails are most common worldwide responsible for affecting 25% of the world population. Fungi are heterotrophic in nature. They are not necessarily harmful they can also be beneficial and help in biodegradation. Harmful fungi include dermatophytes, yeast, and moulds etc. Fungi can cause both superficial as well as invasive infections. Yeasts are not usually harmful except in specific conditions like when host immune system is weakened like in the case of hospitalized patients, or when skin barriers or normal flora is compromised. Fungi can affect mucus membrane of a person as well as nails, skin vagina etc. but the progression of these infections is much worse in case of immunocompromised patients (Kumar, 2018).

1.2. Superficial Candidiasis

Candidiasis is majorly caused by yeast known as *Candida albicans*. It mainly resides in moist areas of the body. It is exhibited as mouth thrush, armpit infections, vaginal thrush, or rashes. Rashed are inflamed, itchy and red in colour (Martins *et al.*, 2014).

1.2.1. Oropharyngeal candidiasis

Typical signs and symptoms are soreness, white patches are most common with erythematous background, bleeding gums and tongue makes it very hard for the individual to eat. This disease is prevalent, especially in geriatric people, as well as those who have received immunosuppression or antimicrobial treatment. It is a significant infectious AIDS consequence and a sign of advanced HIV infection. White plaques indicative of the infection can be seen on the oral mucosa (pseudomembranous candidiasis; On the tongue's surface, this causes the disappearance of tongue papillae (erythematous candidiasis), or the mucosa may appear glazed and erythema can be seen (Hay, 1999).

1.2.2. Vaginal candidiasis (Vaginal thrush)

Vaginal thrush and oral thrush have similar symptoms except that there is white discharge in genital infections along with rashes and pain (Hay, 1999).

1.2.3. Cutaneous candidiasis

Skin candidiasis is frequently restricted to body folds, such as the areas between the fingers or toes. Usually, tiny satellite pustules are located distally to the rash's margin. Candida may result in chronic paronychia (nail-fold infections) (Hay, 2013).

1.3. Epidemiology

Cutaneous candidiasis affects women more commonly than men. It is considered as public health problem all over the world. A study was done in Tehran-Iran to reveal the clinical epidemiology of cutaneous candidiasis Nails scrapings and skin of affected patient's revealed that *C. albicans* was the most common specie responsible for 39.8% of infection followed by *C. parapsilosis, C. orthopisilosis, C. tropicalis* with 32.9%, 10.4% and 7.9% infection prevalence respectively. Candida species are the 4th main cause of bloodstream infection in United States and rates of these infections are high among elderly patients (Ruhnke, 2006; Havlickova *et al.*, 2009).

A study conducted at Quaid-i-Azam international hospital Islamabad in Jan 2014 to Feb 2015 revealed that out of 219 candida isolates the predominant specie was *C. albicans 128 (58*.45%) followed by *C. glabrata, C. tropicalis, C. krusei, C. parasilosis* and so on (Tasneem *et al.*, 2017).

1.4. Eitiology

Small amount of Candida usually resides on the skin of normal person, but because of several factors enlisted below their growth becomes uncontrollable and infection occurs. The main factors responsible for candidiasis are as follow.

Local factors for example those which destroy skin barriers like macerations, ulceration or mucositis caused by radiations. Antibiotic also kill bacteria present on the skin which are not harmful and results in infection. Corticosteroids weaken the immune system. Immune system is also weakened due to various endocrine diseases. In the case of diabetes mellitus level of glucose in body is increased which will result in altering of yeast adhesion and will result in reduction of phagocytosis. Other diseases include Cushing syndrome and hypothyroidism etc. pregnancy and other medical conditions can also increase risk of infection. Chronic candidiasis means re occurring infection and it results due to endocrine or autoimmune diseases. In the case of autoimmune disease like AIDS because of weak immune system T lymphocyte are unable to eradicate the infection via phagocytosis or by using polymorphonuclear cells and

macrophages for killing yeast cells. Patients with primary immune deficiencies for example lymphocytic dysfunction, phagocytic abnormalities, IgA deficiency or severe congenital immunodeficiency are at much higher risk of infection. Conditions due to deficiency of nutrition's for example iron deficiency anaemia or deficiency of folic acid and vitamin B1, B2, B6 or vitamin C will increase the risk of infection to many folds. Other factors include warm weather, poor hygiene conditions, obesity, damp skin, tightly fitted clothes or infrequent undergarment changes etc (Martins *et al.*, 2014; Taudorf *et al.*, 2019). Summary of factors responsible for infection is given in **Table 1.1**.

Table 1.1. Summarized list of factors that trigger cutaneous candidiasis.

Factors responsible for candidiasis	**References**
Local factors e.g., skin maceration	Martins *et al.*, 2014;
Antibiotics, corticosteroids	Martins *et al.*, 2014;
Endocrine diseases like diabetes mellitus	Taudorf *et al.*, 2019
Autoimmune diseases	Taudorf *et al.*, 2019
Primary immune deficiencies e.g., lymphatic abnormalities	Taudorf *et al.*, 2019
Nutritional deficiencies	Martins *et al.*, 2014
Poor hygiene conditions	Taudorf *et al.*, 2019
Obesity	Martins *et al.*, 2014
Damp skin	Martins *et al.*, 2014
Warm weather	Taudorf *et al.*, 2019

1.5. Pathogenesis

Candida exists in different locations of the body and several different adaptive mechanisms help candida to survive in these areas of the body. For example, pH regulated genes are expressed by candida at different pH to survive. pHR1 is expressed to exist at pH 5.5 which is the pH of the skin. To exist at neutral pH pHR2 is highly expressed. *C. albicans* and other species of candida cause infections passing through different stages (De Bernardis *et al.*, 1998).

First step is attachment to the host cell. Host cell has different mechanism to combat infection at this stage, e.g., flushing mechanism or via different substances which are present at the host surface prevents colonization of fungi. The protein Hwp1 helps to form attachment between yeast and epithelium surface.

In **second step** once the yeast cells get embedded to the surface, they will transform into hyphae via the phenomena known as thigmotropism or contact sensing. After hyphae formation next steps is transfer inside the host cells. This also takes place via two mechanisms; firstly, through endocytosis and second is through fungal hydrolases which helps in penetration inside the host cells. Proteases are also released by candida to contribute to spread of infection. Prevention of infection may occur through various mechanism e.g., keratinised surface of host cells via phagocytosis or their innate resistance i.e. activation of T lymphocytes. When candida invades keratinocytes, they will respond via release of chemokines and cytokines. Melanocytes also help in killing the fungi by the release of antimicrobial agents and melanin.

In the **last step** after attachment to biotic or abiotic surfaces biofilms are formed. Biofilms will be formed in such a way that yeast cell will be in lower part and hyphae will be present in the upward site (Odds, 1994; Mathur and Devi, 2017).

1.6. Present Pharmacotherapy

After 1990, number of antifungal agents and classes has been increasing because of rapid development in this field. The drugs are usually compounded in the form of sprays, ointments, creams, and gels etc. because of the non-invasive route they have better patient compliance, and this also bypass first pass effect. Because they do not reach the systemic circulation, side effects from topical treatment are also significantly reduced.

Different classes of antifungal drugs are discussed as follow.

Antifungal medications such as imidazole's, triazoles, and thiazoles are effective against dermatophytes and yeast. It has been demonstrated that they block the enzyme needed to change lanosterol into ergosterol i.e., lanosterol 14-demethylase. Ergosterol in the fungal membrane gradually depletes, leading to fungal membrane dysfunction. The structure of the fungal membrane and its various functions resulted in the inhibition of fungal growth.

Amphiphilic macrocyclic compounds called polyenes have a lot of conjugated double bonds as well as a heavily hydroxylated region on the ring that is opposite the conjugated system. Candida specie but not dermatophytes, are targets for this significant class of medicines. Ergosterol increases the phospholipid bilayer's

mechanical strength, making the plasma membrane denser under typical conditions. This group of drugs binds to ergosterol and causes cell leakage, which leads to cell death.

Allyl amine fungicides are used to treat fungal diseases of the skin and nails. Only dermatophytes are resistant to them. These are non-competitive, reversible antagonists of the squalene epoxidase enzyme, which initiates the production of ergosterol by converting squalene to squalene-2,3- epoxide. Squalene build-up in the cell membrane is harmful to the cell, producing imbalance of pH and membrane protein dysfunction.

By specifically targeting the microtubule, the antifungal agent nucleoside prevents cell division. This prevents the formation of the mitotic spindle or suppresses DNA transcription. Echinocandins are a group of drugs that inhibit the synthesis of cell walls by blocking the enzyme glucan synthase. The hydroxy pyridone antifungal ciclopirox disrupts a variety of processes, including fungal respiration, cellular membranes integrity, and active membrane transport.

As tolnaftate, a thiocarbamate antifungal, blocks fungi squalene epoxidase, griseofulvin attaches to polymerized microtubules and prevents fungi from going through mitosis. Antimycotic medicines' diverse mechanisms, as stated above, give protection against a wide spectrum of fungi, implying that infections caused by them can be effectively and successfully treated (Hay, 2013; Mathur and Devi, 2017)

1.7. Transethosomes (TESs)

Nanocarriers improve drug pharmacokinetics and biodistribution to the target organ, resulting in increased efficacy. The drug's toxicity is decreased because it accumulates at target areas rather than in healthy tissues. As a result, nanocarriers enable drug delivery that is both continuous and controlled. Many varieties of ultra-deformable vesicles have been successfully created for pharmacological and cosmeceutical applications, including liposomes, ethosomes, transferosomes, and, more recently discovery is, TESs. Liposomes can’t cross stratum corneum. But more UDV vesicles like transferosomes and ethosomes contain edge activator and ethanol respectively. Both these chemicals are penetration enhancer and make them highly elastic and they can cross the pores of the skin which are much smaller than their own diameter (Bajaj *et al.*, 2021).

TESs are the hybrid of transferosomes and ethosomes firstly introduced by Song et al in 2012 and are distinguished by a high ethanol content (up to 30%) combined with an edge activator. They contain advantages of both ethosomes and transferosomes. They are highly elastic, and they have irregular spherical form. They can encapsulate both low molecular weight and high molecular weight medicines. TESs are thought to be superior to other formulations because of their high drug encapsulation efficiency. It has the power to change its shape and form and they can enter deep layers of the skin (Song *et al.*, 2012).

1.7.1. Structure of TESs

They are lipid-based vesicles. They mainly contain phospholipids, edge activator (surfactant), ethanol and water. Main role of phospholipid which are non-ionic surfactant is to transport the molecules of drugs across the layers of skin. Phospholipid can easily interact with stratum corneum, and they hydrate the tissues. They have polar (hydrophilic) heads and non-polar (lipophilic) tails. Examples of phospholipids are soya phosphatidylcholine, dipalmitoyl phosphatidylcholine, Di stearoyl phosphatidylcholine. The next important component of TESs is edge activator (biocompatible surfactant) e.g., tween 80, span 80, sodium deoxycholate etc. Their main role is enhancement of penetration and improvement of flexibility of the structure. The unique component present in TESs is alcohol. Ethanol deforms layers of the skin making TESs highly flexible. Water or buffer (pH 7.4) helps to form bilayer structure along phospholipids **Table 1.2** explains major components of TESs along with their uses (Mohammed and Al Gawhari, 2021). **Figure 1.1** shows structure of TESs.

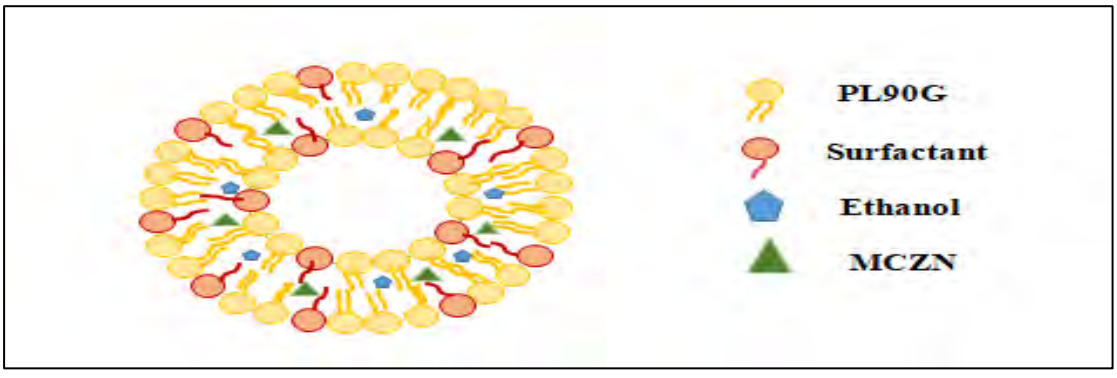

Figure 1.1. Structure of TESs.

Table 1.2. Composition of TESs.

Composition	Examples	Uses
Phospholipid	Soy phosphatidylcholine, phospholipon90®G, dipalmitoyl phosphatidylcholine,	Helps in vesicle formation
Surfactant	Tween 80, tween 20, span 80, sodium cholate, sodium deoxycholate, oleic acid	Improves flexibility and enhance penetration
Alcohol (30-40%)	Ethanol	Helps in softness of membrane of vesicles
Buffering agent	Phosphate buffer saline pH 7.4	Works as a hydrating agent

1.7.2. Advantages of TESs

- Phospholipids are one of the major components which makes them biocompatible and biodegradable.
- Very high entrapment efficiency in the case of lipophilic drugs entrapment is increased up to 90%.
- They prevent degradation of drug and release the drug in sustain and control manners.
- Their flux rate is very high so they can easily cross barriers of the skin.
- They can be given topically as well as systemically.
- They can encapsulate drug with high and low molecular weights.
- Use of TEs is non-invasive. Patient compliance is very high because they can easily be administered as semisolid dosage forms like gels, creams etc.
- Most stable among all ultra-deformable vesicles (Mohammed and Al Gawhari, 2021).

1.7.3. Mechanism of permeation of TESs

Three layers of the skin are epidermis, dermis, and hypodermis. Epidermis is the outer most layer made of keratinocytes and is the major barrier for the drug absorption. Stratum corneum is the non-viable epidermal layer. Then comes dermis made up of connective tissues. Hair follicles, sebaceous gland and sweat glands are present in this layer. Hypodermis consists of sebaceous fat tissues. There are two mechanisms by which TESs pass through these three barriers of the skin. Ethanol when pass through stratum corneum it disrupts phospholipids and fluidizes lipids. Gaps between corneocytes increases which results in increased penetration resulting in gradual release of drug in these layers. Secondly edge activator works by disruption of intercellular

lipids and hydrophilic pores are widened, then medication is released gradually. But edge activator alone is not capable of transferring the drugs in deep layers. But both edge activator and ethanol increase elasticity and fluidity of TESs. Fluidity of lipid membrane cause decrease in size and elasticity makes it capable to alter or change its shape and pass-through narrow pores which are much less in diameter. After passing through epidermis TESs moves to dermis layer (Simõe, 2015).

1.7.4. Methods of preparation of TESs

At both the pilot plant and industrial size, TESs are simple to create and scale up without the use of specialized technology. To improve skin penetration, different technologies are employed to create small vesicles, which are then put into gels or creams. The approaches listed below are some of the most regularly employed.

1.7.4.1. Cold method for preparation of TESs

According to this procedure, lipids are solubilized in ethanol with constant stirring at normal room temperature, then edge activator is added, and the above mixture is heated to 30°C while being vigorously stirred. The mixture is then stirred in an enclosed pot for 5 minutes. The water is added to the alcoholic mixture gradually in a fine stream after being boiled in a separate container to 30°C. TESs size is also decreased with sonication. The formulation is then stored in a refrigerator (Kumar *et al.*, 2016).

1.7.4.2. Hot method for preparation of TESs

A colloidal solution is created by dispersing phospholipid in water and heating it in a water bath to 40°C. Glycol and ethanol are kept at a constant 40°C temperature. The aqueous phase is combined with the ethanol and glycol-containing phase while being stirred for 7 to 10 minutes. The drug can dissolve in water or ethanol depending on whether it has hydrophilic or hydrophobic qualities. The process is conducted at a constant temperature of 40 °C. Sonication causes the TESs to shrink in size (Kumar *et al.*, 2016).

1.7.4.3. Mechanical dispersion / thin film hydration method for preparation of TESs

Lipid and surfactant are combined and dissolved in ethanol in a clean, dry, round-bottom flask. The thin-film hydration and ultrasound homogenization together improved this process. Above the lipid transition temperature, a rotary evaporator is used to create a thin lipid film. By holding it overnight under a vacuum, extra organic

solvent is eliminated. The film is hydrated by rotation at 60 rpm while immersed in a phosphate buffer solution with a pH of 6.5 and 10% v/v ethanol. The formulation is then supplemented with the drug. To make them smaller, TESs are sonicated. TESs were homogenised for five minutes using sonification. Using a 0.22 m filter to filter TESs was done lastly (Mohammed and Al Gawhari, 2021).

1.8. Miconazole Nitrate (MCZN)

MCZN is an antifungal drug which belongs to imidazole class. Basically, azoles are the class of antifungals which further classify into azole and imidazole based upon the number of nitrogen atoms present in the structure. Imidazole's contain two nitrogen atoms in their structure. Imidazole's are mainly known for treating superficial fungal infections (Fothergill, 2006). Conventional dosage forms of MCZN are available in the market but these dosage forms have various shortcomings and side effects (Firthouse *et al.*, 2011).

For the topical treatment of infections, the main problem is to cross the skin barriers to reach deep skin layers. In case of MCZN that is insoluble in water and its octanol water partition coefficient is 6.25 that means that this drug has very poor skin penetration (Pandit *et al.*, 2014).

1.8.1. Mechanism of action of MCZN

MCZN is unique drug among azoles class. The discriminating factor of MCZN is its mechanism of action. It is used to treat various infections especially those that are caused by the overgrowth of Candida species.

Three mechanisms of actions followed by MCZN are as follow.

1.8.1.1. Inhibition of ergosterol Synthesis

The primary mechanism of action which MCZN shares with other azoles is the inhibition of production of ergosterol which is important component of fungal cell membrane. Basically, MCZN inhibits enzyme named CYP450 14α lanosterol demethylase as shown in **Figure 1.2.** This enzyme is responsible for converting lanosterol to ergosterol by the elimination of methyl groups. As the result of its inhibition methylated sterols tend to accumulate in cell membrane and integrity of cell membrane, its permeability along with the action of membrane bound enzymes gets

affected. This action will in turn cause leakage of phosphate, cations and low molecular weight proteins (Mathur and Devi, 2017).

1.8.1.2. Production of ROS

The second mechanism of action that makes MCZN superior to other azoles is production of ROS. Despite inhibition of ergosterol azoles are not completely static in nature. They can slow down fungal growth but they need assistance from immune system in order to completely exterminate infection (Kobayashi *et al.*, 2002). Production of ROS is completely independent pathway from ergosterol inhibition. MCZN inhibits peroxidase enzyme that leads to the accumulation of hydrogen peroxides in the cell to a toxic level resulting in necrosis or cell death. This ability of MCZN to disturb peroxidative and oxidative enzymes activities makes it capable of fungicidal effect. And this is the reason for less fungal resistance of this drug (Piérard *et al.*, 2012). A explained in **Figure 1.2**.

1.8.1.3. Production of farnesol

The formation of farnesol in *Candida* spp. that are sensitive is another example of how intricate the MCZ's mode of action is. An extracellular quorum-sensing molecule is farnesol that is produced by *C. albicans*. Farnesol build-up above a certain point result in inhibition of the yeast-to-mycelium transition and limits the proliferation of budding yeast. (Piérard *et al.*, 2012).

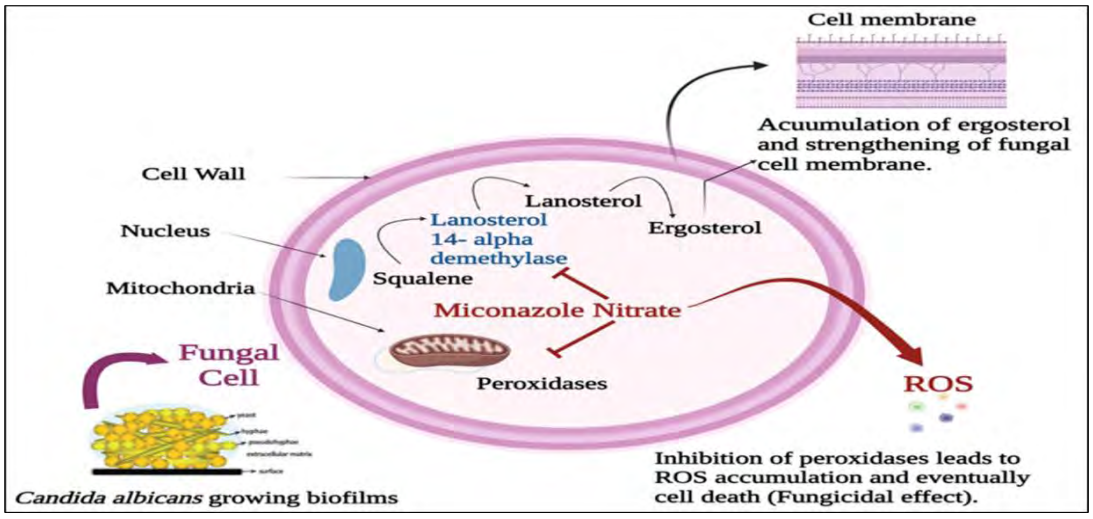

Figure 1.2. Mechanism of action of MCZN (created via Bio render).

1.9. Rationale

The rationale of this ultra-deformable vesicle system was to enhance penetration and to improve antifungal potential for the treatment of cutaneous candidiasis.

1.10. Aim and Objectives

The aim of current study was the development of Miconazole Nitrate transethosomes (MCZN TESs) and chitosan-based Miconazole Nitrate loaded transethosomal gel (MCZN TESs Gel) for the treatment of cutaneous candidiasis.

The objectives of this study were.

- To optimize and characterize MCZN TESs and MCZN TESs Gel.
- *In vitro* and ex vivo evaluation of MCZN TESs and MCZN TESs Gel.
- *In vivo* evaluation and investigation of antifungal potential of MCZN TESs Gel.

CHAPTER 2

MATERIALS AND METHODS

2. MATERIALS AND METHODS

2.1. Chemicals and Reagent

MCZN was kindly gifted by Valor pharmaceuticals Islamabad. Phospholipon® 90G (PL90G) and Span 80 (S 80) were procured from sigma aldrich. Chloroform, methanol, and ethanol were purchased by BDH laboratory supplies, England. Di-sodium hydrogen phosphate ($Na_2HPO_4.2H_2O$) and potassium di-hydrogen phosphate (KH_2PO_4) were obtained from Merck, Germany. Sodium chloride (NaCl), sodium hydroxide (NaOH) was purchased from sigma Aldrich. Acetic acid and Chitosan were procured from sigma Aldrich. Dialysis membrane (Dialysis tubing with MWCO 12 to 14 kDa) was procured from the Medicell membranes Limited (London UK).

2.2. Instruments and Apparatus

Rotary evaporator (Heildoph Instruments GmbH CO., Germany), Weighing balance (Ohaus corporation, PA 214C, USA), Hot plate multi stirrer (MAGIK, MG-855), Water distillation apparatus (IRMECO GmbH IM50, Germany), Centrifuge machine (Hermle, GmbH Z326K, Germany), Agilent 8543 Ultraviolet-Visible Spectrophotometer (Agilent technologies, United States), Bath sonicator (Elmasonic GmbH, E60H, Germany), Probe sonicator (Misonix-XL-2000 series), pH meter (Bante instruments, PHS 25GW, Chicago, USA), Refrigerator (Panasonic MPR-161D H, Japan), Oven (Memmert, INB200, Germany), Lyophilizer (Christ alpha 1-2 LD plus, Germany), FTIR spectrometer (Nicolet, model Magna-IR spectrophotometer 550), DLS instrument (Brook heaven instrument corporation, USA), Malvern Zeta sizer, Franz diffusion cell (Model T9-CB-71026, Make: PermeGear, Inc. USA), funnel, beakers, petri dishes, pipettes and stirrers, falcon tubes, glass vials, micro spatula, syringe filters, volumetric flask, Eppendorf tubes (Sigma Aldrich, USA).

2.3. Methods

2.3.1. Formulation of solutions

2.3.1.1. Phosphate Buffer Saline (PBS pH 7.4)

100 ml volumetric flask was taken in which accurately measured 238 mg of $Na_2HPO_4.2H_2O$, 800 mg of NaCl, 19 mg of KH_2PO_4 were dissolved in small quantity of water. After complete dissolution of salts volume makeup was done to 100 ml with

distilled water (Nurahmanto, 2013).

2.3.1.2. Phosphate Buffer Saline (PBS pH 5.5)

In a small quantity of water dissolve 8.09 g of $Na_2HPO_4.2H_2O$, and 1.36 g of KH_2PO_4 and makeup the final volume up to 400 ml with distilled water.

2.4. Standard Calibration Curve

2.4.1. Standard calibration curve of miconazole nitrate

Methanol was selected as the most suitable solvent for the preparation of curve of MCZN. Because this lipophilic drug had the maximum solubility in this solvent. First, standard stock solution of 100 µg/ml was prepared by dissolving 1 mg of MCZN in 100 ml of methanol. Then by using this stock serial dilutions were prepared.

For the calculation of volume of methanol following equation was used.

$C_1V_1=C_2V_2$
C_1= Concentration of stock solution V_1= Vol. of stock solution
C_2= Concentration of succeeding dilution V_2= Vol. of succeeding dilution

For the analysis of prepared dilutions UV-Spectrophotometer was used at the wavelength of 272 nm (λmax) (Cavrini *et al.*, 1989) . all the values of absorbance's for each dilution were recorded and calibration curve was plotted between concentration and absorbance. R^2 value was obtained along with linear regression equation.

$y = mx + c$
y = absorbance m = slope
x = unknown conc. of drug c = intercept

2.4.2. Calibration curve of MCZN in PBS (pH 7.4)

Calibration curve was made at pH 7.4 to analyse release pattern of TESs in blood. All the values obtained were analysed using UV-Spectrophotometer at 272 nm.

2.4.3. Calibration curve of MCZN PBS (pH 5.5)

To check the release behaviour of MCZN at pH 5.5 i.e., the pH of skin calibration curve was formulated. Different dilutions were prepared and checked at UV-Spectrophotometer at the wavelength of 272 nm.

2.5. Method of Preparation of TESs

2.5.1. Method of preparation of blank TESs

Thin film hydration method was used for the preparation of TESs with slight changes in the method. First, PL90G along with S 80 were dissolved in organic solvents i.e., methanol and chloroform (1:1). The mixture was transferred into rotary flask and was evaporated under vacuum to form a thin film. After the formation of thin film hydration was done using aqueous phase consisting of PBS 7.4 and ethanol (7:3) for one hour at 60°C and 100 rpm. After the hydration formulation was sonicated for 5 minutes and then extrusion was done to obtain small vesicles. This method is explained in **Figure 2.1** (Song *et al.*, 2012; Ahmed *et al.*, 2021).

2.5.2. Method of preparation of MCZN TESs

Same thin film hydration method was used for the formulation of drug loaded TESs. Drug was lipophilic so was added into organic phase along with lipid and surfactant. After formation of thin film hydration was done for one hour at 60 °C and 100 rpm. After sonication and extrusion, vesicles were obtained (Song *et al.*, 2012; Ahmed *et al.*, 2021).

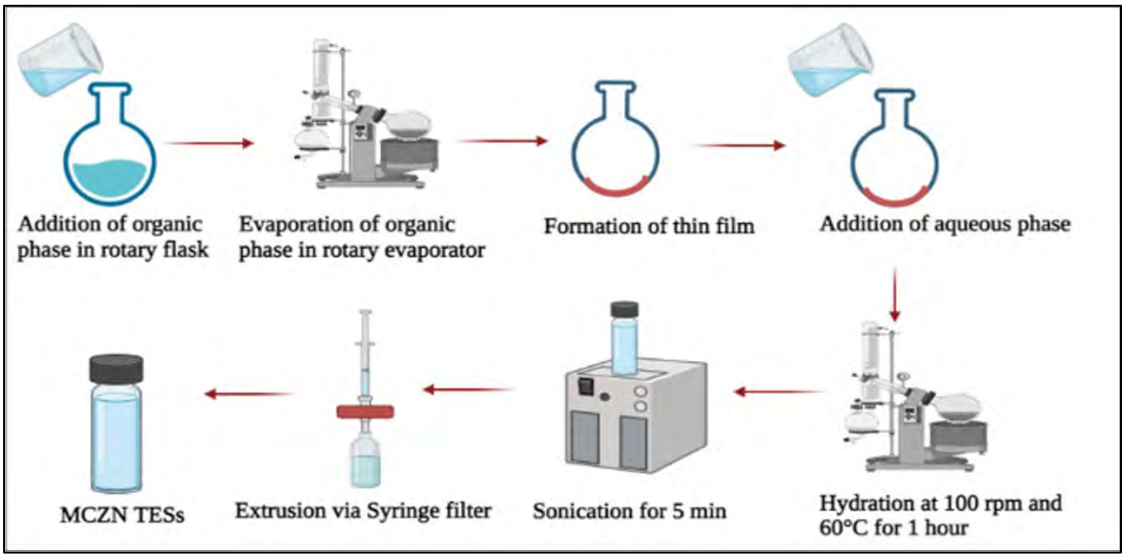

Figure 2.1. Method of preparation of MCZN TESs via thin film hydration method (created via Bio Render).

2.5.3. Parameters adjusted during pre-optimization

To create stable TESs, various parameters were investigated. These included the amount of lipid, the amount of the edge activator, the ratio of the organic solvents, the

amount of the drug, and the volume of hydration under study. Phase separation, physical characteristics, and formulation sedimentation all played a role in the ultimate decision of which range of these parameters to use.

Using different amounts of lipid and S 80 blank TESs were initially optimised. In every composition, the final volume of hydration medium remained consistent. According to a smaller particle size (PS), a smaller polydispersity index (PDI), and a higher zeta potential (ZP), the optimised blank TESs were selected.

2.5.4. Optimization of MCZN loaded TESs by Box-Behnken Design

After pre optimization done on TESs the parameter that affected passage of TESs were selected. It was observed that noticeable difference occurred when the quantity of drug, PL90G and S 80 were changed. Based on the data collected from pre optimization these three factors were selected and constraints were set accordingly. For the main optimization a two-level three-factor, Box-Behnken Design was used employing software known as Design Expert® (Version 12, Stat-Ease Inc., USA). Design Expert® gave total 13 experimental runs. There were three independent variables i.e., lipid, surfactant, and drug. And four dependent variables were PS, ZP, PDI and entrapment efficiency (EE) (Alam *et al.*, 2017).

2.5.5. Freeze drying of TESs

Formulation was centrifuged for three hours. After centrifugation supernatant was discarded. Pellets were collected and resuspended in 3ml PBS and incubated at -80 °C for 24 hours. Christ alpha1-2 LD plus lyophilizer was used to lyophilize the frozen materials. The resulting pellets were stored for later use at 4 °C (Abdelwahed *et al.*, 2006).

2.6. Preparation of Chitosan Gel

2.6.1. Preparation of acetic acid solution

1% acetic acid solution was formulated. 100 ml volumetric flask was taken firstly 1 ml of acetic acid was dissolved in little amount of water and then volume was made up to 100 ml (Alsarra, 2009).

2.6.2. Preparation of blank chitosan gel

Based on physical consistency of chitosan gel different concentrations were prepared. 1%, 2%, 2.5%, 3% (w/v) gels were prepared. Among them 2% (w/v) chitosan gel was

selected. For gel preparation 100 mg chitosan was dissolved in 3 ml volume of 1% acetic acid and continuously stirred. After dissolving chitosan 2 ml of PBS was added in chitosan solution. Stirring was done continuously until a homogeneous mixture was formulated (Alsarra, 2009).

2.6.3. Preparation of MCZN TESs Gel

For drug loaded gel preparation 100 mg chitosan was dissolved in 3 ml volume of 1% acetic acid and continuously stirred. After dissolving chitosan 2 ml of PBS having pellets of MCZN TESs dispersed in it were added in chitosan solution. Stirring was done continuously until a homogeneous mixture was formulated (Alsarra, 2009). **Figure 2.2** shows method of preparation of gel.

Figure 2.2. Method of preparation of chitosan gel.

2.6.4. Optimization of chitosan gel

Multiple concentrations of chitosan gels were prepared as given in **Table 2.1** and were evaluated. 2% chitosan gel was selected as optimized formulation.

Table 2.1. Optimization parameters of chitosan gel.

Conc. of chitosan (%)	Amount of chitosan (mg)	Volume of PBS (ml)
1	75	5
2	100	5
2.5	125	5
3	150	5

2.7. Characterization of TESs

2.7.1. Particle size analysis

Zeta-sizer (Malvern zeta sizer ZS 90) was used to measure the prepared vesicles size by employing dynamic light scattering (DLS) technique. Preparation of sample was done by taking 10µl of MCZN TESs formulation and diluting it in 1ml of distilled water and then sample was placed in zeta sizer for analysis. Analysis was carried out three times, and results were presented as mean ± S.D (standard deviation) (Ahmed *et al.*,

2020).

2.7.2. Polydispersity index

PDI of the formulation was computed using the same method explained in section 2.7.1. PDI measures the uniformity and homogeneity of the vesicles in the formulation; the optimal range is 0–1. Values that are nearer to 0 indicate a formulation with less polydispersity and more monodispersity (Ahmed *et al.*, 2020).

2.7.3. Zeta potential

The stability of the formulation is correlated with the zeta potential, which denotes the existence of charge on the surface of vesicles. If zeta potential is low, it indicates that particles are close to one another and that there is a greater likelihood of aggregation, which makes the system less stable. The higher the value of zeta potential, the more stable the system is. The zeta potential of TESs was determines using method explained under section **2.7.1**. (Ahmed *et al.*, 2020).

2.7.4. Entrapment efficiency

For calculating EE indirect method was used. MCZN TESs were centrifuged for three hours at -4°C 13500 rpm. After completion of centrifugation supernatant was collected and analysed by making different dilutions using UV-Spectrophotometer at 272nm (λ max) (Bhalekar *et al.*, 2009).

UV-spectrophotometer was used for determination of drug entrapped in TESs. Following formula was employed for calculations.

$$\% \text{ Encapsulation efficiency} = \frac{\text{Total drug} - \text{Free drug} * 100}{\text{Total drug}}$$

2.7.5. Fourier transform infrared spectroscopy (FTIR) analysis of optimized MCZN TESs

To examine the interactions between various applied substances, FTIR analysis was performed. To ascertain how these substances interact with one another, drug, TESs formulation, and PL90G analyses were carried out using FTIR spectrophotometer (Nicolet, model Magna-IR spectrophotometer 550). A frequency range of 4000-400 cm^{-1} wavenumbers was used for the FTIR investigation (Bhalekar *et al.*, 2009).

2.7.6. Differential scanning calorimetry (DSC) analysis of optimized MCZN TESs

Thermal analysis was performed for pure miconazole nitrate drug, PL90G and lyophilized form of miconazole nitrate loaded TESs using differential scanning calorimeter. The temperature range for the DSC thermograms was 0 to 250 °C, with a scanning speed of 10 °C/min (Bhalekar *et al.*, 2009).

2.7.7. Deformability index (DI) and elasticity study of MCZN TESs vesicles

For testing the deformability of the lipid bilayers of the optimised MCZN TESs, extrusion technique was used. MCZN TESs was designed to pass through membrane filters with the 100 nm of pore size. Assessments of vesicle size prior to and after extrusion was done. A calculation of deformability was then made using the following equation (Rabia *et al.*, 2020).

$$Deformability\ index = \frac{Size\ after\ extrusion\ of\ MCZN\ TESs\ vesicles}{Size\ before\ extrusion\ of\ MCZN\ TESs\ vesicles}$$

$$\%\ Deformability = \frac{Size\ after\ extrusion\ of\ vesicles}{Size\ before\ extrusion\ of\ vesicles} \times 100$$

Shape changes during stress is known as elasticity and is measured by following formula (Rabia *et al.*, 2020).

$$Elasticity = \frac{Size\ after\ extrusion}{Pore\ size}$$

2.8. Characterization of MCZN TESs Gel

Spreadability, rheology, gel pH, drug content, and homogeneity are some of the factors that were chosen to characterise TESs. Chitosan gel was chosen based on the physiochemical characteristics and recommended ranges for gels.

2.8.1 Gel clarity, uniformity, and drug content

By visual inspection, the homogeneity, consistency, and clarity of each chitosan gel formulation was evaluated. To check the homogeneity, a small amount of gel was inserted between the index finger and thumb. For drug content measurement,5 mg of gel sample was dissolved in 5 ml PBS, and the gel solution was kept for 24 hours and afterwards it was shaken 30 using magnetic stirrer. After that, solution was filtered and used to measure the drug content by UV- Spectrophotometer at 272 nm. Drug content of formulations was assessed in the triplicate (Borse *et al.*, 2020).

2.8.2. pH of Gel

By mixing 1 g of MCZN TESs gel with 20 ml of pure water, the pH of the gel was calculated. By inserting the pH meter's electrode into the gel solution and measuring the result, the pH of the solution was noted. Three times of each reading were taken, and the mean and standard deviation were calculated (Borse *et al.*, 2020).

2.8.3. MCZN TESs Gel rheology

To study the effect of shear rate, viscosity was recorded at different speed and flow behaviour of chitosan based MCZN TESs gel was determined. To perform this experiment Brookfield viscometer was used. Viscosity dependent or independent behaviour on applied stress was noted (Salim *et al.*, 2020).

2.8.4. Spreadability study

Glass slide method was used. A circle with a diameter of 2 cm was placed on a slide to test the gel's ability to spread, and 0.5–1 g of gel was then added to the circle. Then, a second glass side with a weight of about 0.5 kg was placed on the first slide. Leave it for 5 minutes to examine its extreme spreadability, and after that, the diameter rise was seen. This equation was utilised to calculate spreadability (Qindeel *et al.*, 2019).

$$\% \text{ Spread area} = \frac{\text{Final area after spreading} \times 100}{2\text{cm}}$$

2.9. *In Vitro* Drug Release Profile

2.9.1. *In vitro* release study of formulations

At pH 5.5, the *in vitro* release pattern of MCZN TESs, miconazole nitrate dispersion (MCZN dispersion), MCZN TESs gel, Marketed Gel, and drug gel (MCZN Gel) was carried out in triplicate. This experiment was carried out using mechanical shaker water bath equipment with a few minor changes. For MCZN TESs and MCZN dispersion pellets carrying 2 mg of medication were transferred into a dialysis bag after being dissolved in 3 ml of phosphate buffer. MCZN TESs gel was prepared by placing predetermined quantity of TESs in chitosan solution. In case of MCZN Gel 2 mg of MCZN was placed in chitosan solution and gel was formulated. So, drug quantity was kept equal in all the formulations. The dialysis bags were then put in a beaker with 50 ml of PBS that had pH values of 5.5. The mechanical shaker's temperature and speed were both set at 37 ± 2 °C. A certain time interval of 0.25, 0.5, 1, 2,3, 4, 6, 8, 12 and 24 hours was chosen for sampling. To keep the sink condition, 1 ml of sample solution

was withdrawn and replenished with an equal amount of buffer to maintain sink condition. A 24 hours experiment was conducted and after completion of this 24 hours cycles all the collected sample solutions were analysed at UV- Spectrophotometer at 272 nm. *In vitro* release graph was created by plotting the data between time and % cumulative release (Rachmawati *et al.*, 2013).

Formula for calculating cumulative release is as follow.

$$Qn = Vr * Cn + \sum_{i=D}^{n-1} Vs * Ci$$

Qn = Cumulative amount of drug release at sample nth time
Cn = Concentration of drug released in medium at sample nth time
Ci = Concentration in acceptor medium at sample ith time
Vr = Volume of acceptor medium
Vs = Volume of sample withdrawn from the medium

2.10. Kinetic Drug Release Study

Applications of mathematical models to drug release characteristics are known as drug release kinetics. These mathematical representations show how the drug releases in various media. The information gained from these models can then be extrapolated to determine the drug's *in vitro* release from the nanoparticles. To describe the releasing process, various mathematical models have been constructed (Nurhan, 2010).

2.10.1. Zero order release kinetics

Uniform drug release from formulation is predicted by the zero order release model. A straight line is obtained from a graph of zero order between cumulative drug release and time. Zero order signifies that the medication release pattern is unaffected by concentration. The equation below serves as a representation.

$$W = k_1 t$$

W = cumulative drug release t t= Time in hours
k_1 = zero order release kinetics

2.10.2. First order kinetics

A first order kinetic graph is created between the log of the amount of substance left and the passage of time. It shows that the drug release pathway depends on concentration. The following equation represents first order kinetics.

$$\ln (100-W) = \ln 100 - k_2 t$$

k_2 = First order release kinetics

2.10.3. Higuchi model

The Higuchi model graph was used to display the relationship between drug release rate and square root of time. Release is said to follow a diffusion process based on Fick's law, which is time-dependent in accordance with the Higuchi model. Below is the equation used to investigate the Higuchi model.

$$W = k_4 t$$

k_4 = Higuchi dissolution rate constant

2.10.4. Korsmeyer-Peppas

The KP model's graph, which compares log percent of drug release to log time in hours, describes the diffusion process by which drugs diffuse continuously from formulations. The korsmeyer-Peppas model's equation is

$$M_t/M_\infty = k_5 t^n$$

M_t/M_∞ = fraction of drug release

k5 = Korsmeyer peppas rate constant

n = diffusion exponent for drug release

2.10.5. Hixon Crowell model

This release model explains the drug release process using a variety of mechanisms, including dissolution, erosion, and diffusion.

2.11. Ex Vivo Skin Permeation and Skin Deposition Study

2.11.1. Preparation of rat skin

The permeation experiments used skin from albino rats. There are several procedures involved in getting rats skin ready for the permeation study. Rats were slaughtered and their entire abdomen skin was removed using chloroform as the initial stage in the preparation process. The skin was then soaked in hot water for at least 20 minutes to remove all the abdominal fat after all skin hair had been removed with a razor.

Following that, skin was either preserved in 10% formalin or in a freezer at -300 °C. Skin was soaked in phosphate buffer for 20–30 minutes prior to the experiment.

2.11.2. Franz diffusion cell

The permeation investigation was conducted using the Franz diffusion cell (Model T9-CB-71026, Make: PermeGear, Inc. USA). Between the donor and receptor compartments, skin was positioned. For this experiment, four different types of cells were used. MCZN TESs, MCZN TESs Gel, MCZN Gel and Marketed Gel were tested. 1 ml of formulation and 1 g of gel was applied on the skin at the donor chamber, and the receptor chamber's rotation speed was adjusted at 500 rpm while it contained 5 ml of phosphate buffer (PBS 7.4) simulating blood environment. From the tested formulation a sample volume of 1 ml was taken out at specified time intervals and replaced with the same volume of phosphate buffer solution. Furthermore, the apparatus's temperature was held constant at 32 ± 0.5 °C throughout the whole experiment. Samples were analysed using UV- spectrophotometer at the wavelength of 272 nm. Finally graph of %drug permeation vs time was plotted using GraphPad prism v.9.0. Steady state flux (Jss) (µg/cm^2/h), enhancement ratio (ER) were calculated according to previously published data (Andrade *et al.*, 2014).

Equation used for the calculation of permeation is as follow.

$$Qn = Cn * Vr + \sum Ci * V/A$$

Qn = At the time of the nth sample, the total amount of drug penetrated per unit area.

Cn = Drug concentration in receptor fluid at the time of nth sample.

Vr = Receptor chamber volume

$\sum$Ci = sum of drug concentration in receptor fluid before the time of nth sample (at the time of ith (n-1) sample)

V = volume used for the withdrawal of sample

A = Permeation area of Franz diffusion cell (0.77cm^2)

To calculate steady state flux (Jss) (µg/cm^2/h) following equation was used.

$$Jss = \frac{Amount\ of\ drug\ permeated}{Time}$$

Equation used for calculating enhancement ratio (ER) is as follow.

$$ER = \frac{J_{SS}\ of\ formulation}{J_{SS}\ of\ pure\ drug\ gel}$$

2.11.3. Skin deposition study

After completing permeation studies for 24 hours skin deposition studies were performed on the same rat skin. All the skins were removed from the Franz diffusion apparatus and were washed with PBS. After washing skins were dried using cotton swab to dry and remove any formulation present on the surface of the skin. Tape stripping method was used to separate stratum corneum. 20 pieces of cell ophane tape were used. The remaining skin was analysed on UV-spectrophotometer by firstly chopping the skin into small pieces than skin was homogenized and to extract the drug completely from the skin it was sonicated in methanol. And then centrifugation was done at 1000 rpm for 15 minutes. Then supernatant was taken to determine the total drug present in epidermis/ dermis. For analysing the total drug in stratum corneum same procedure was applied on tapes (Wavikar and Vavia, 2013; Haq and Michniak-Kohn, 2018).

2.12. Skin Irritation Studies of MCZN formulations

Draize skin irritation test is based upon observing erythema and edema on the testing area and then grading them based upon their severity (Nawanopparatsakul, 2005). The Bioethical Committee of Quaid-I-Azam University Islamabad approved handling protocol used for this experiment (Protocol No: **BEC-FBS-QAU2022-380)**. Animal used for this study were purchased from National Institute of Health (NIH). Three groups of rats—one each of normal control, 0.8% formalin control, and MCZN TESs gel group—each contained three rats. After shaving the rats' dorsal side, a formulation-loaded gel was applied to the skin. The rats were then monitored for edema, erythema, and any other symptoms for 72 hours (Castro *et al.*, 2011; Shokry *et al.*, 2018).

2.12.1 Evaluation of skin structure

After treating the skin with MCZN TESs gel FTIR analysis was carried out to confirm any change in the lipid alignment of skin structure caused by applied formulation (Batool *et al.*, 2021).

2.13. *In Vitro* Antifungal Assay for MCZN

2.13.1. Preparation of sabouraud dextrose agar (SDA) media

Antifungal activity was done to check efficacy of MCZN TESs gel, MCZN gel and marketed gel against *Candida albicans.* SDA media of about 20 ml was prepared by dissolving the media in distilled water. Heating was done with frequent stirring and boiling was done for 15 minutes. Autoclave at 121°C for fifteen minutes. After cooling it to about 45 to 50°C prepared media was poured into petri dishes (Ni and Streett, 2005).

2.13.2. Agar well diffusion method

Agar plate surface was inoculated by spreading microbial inoculums of *C. albicans* (obtained from Department of Microbiology Quaid-i-Azam University Islamabad) on the surface of SDA media. After the culture of *C. albicans* was ready holes were created on the plate aseptically by using sterile syringe and desired volume of samples was introduced into the wells. Incubation of plates was done for 48 h at 25 °C. The antimicrobial agent diffusion occurred in the agar media and growth of microbes was retarded. After 48 h measuring of diameter of zone of inhibition was done using scale. Triplicate readings were taken in mm units (Sriram *et al.*, 2019; Ahmed *et al.*, 2021).

2.14. *In Vivo* Antifungal Evaluation of MCZN TESs gel

2.14.1 Immune system suppression of rats

The Bioethical Committee of Quaid-I-Azam University Islamabad approved handling protocol used for this experiment (Protocol No: **BEC-FBS-QAU2022-380)**. Albino rats having the weight between 180 to 210 g were obtained from National Institute of Health (NIH). Before being assigned to the experimental treatment, all animals were given a week to acclimate in standard animal facility settings. To compare the effectiveness of the MCZN TESs Gel with MCZN Gel and Marketed Gel (Daktarin) in treating deep fungal infection, immunosuppression was used to create a heavy cutaneous infection. Intravenous methylprednisolone (5 mg/kg) was administered to rats for three days, suppressing their immune systems, before a fungus infection was introduced (Song *et al.*, 2012).

2.14.2. Preparation of culture of *C. albicans*

On SDA media, *C. albicans* were left to grow for 48 hours at 30 °C. The cells were then gathered, cleaned, and were suspended in sterile saline to achieve an ultimate concentration of 10^7 CFU/mL (Song *et al.*, 2012; Conti *et al.*, 2014).

2.14.3. Induction of candidiasis in rats

About 4 cm^2 of hair were removed from each rat to prepare them. In the centre of the shaved area, 100 µL of a Candida albicans suspension 10^7 CFU/mL were intradermally injected into each rat. The minor edema was massaged out of the injection site. After 72 hours, the fungal infection was found (Song *et al.*, 2012).

2.14.4. Design of the experiment

Rats were divided in to five groups each group contain six animals in total. Group 1 served as negative control in which no induction and treatment was given. Group 2 was named as positive control in which infection was induced only but no treatment was given. Group 3 was MCZN TESs Gel treated group. Group 4 was Marketed Gel treated group and Group 5 was MCZN Gel treated group. Group 3, 4 and 5 were given treatment topically for 7 to 10 days until the infection was cured (Song *et al.*, 2012).

Table 2.2. Design of the experiment.

Group No	Group name	Induction	Treatment
1	Negative control	×	×
2	Positive control	✓	×
3	MCZN TESs gel treated	✓	✓
4	Marketed gel treated	✓	✓
5	MCZN gel treated	✓	✓

2.14.5. Clinical observation of rats

Before and throughout the tests, all rats were monitored to spot any clinical signs of a fungus infection. Rashes, cracking, scaling, and erythema were among the symptoms that were seen and noted (Conti *et al.*, 2014; Qushawy *et al.*, 2018).

2.14.6. Histopathological analysis

Rats were mildly sedated with ether before being slaughtered at the completion of the tests. The damaged area's skin was excised, fixed with formaldehyde at a 10% concentration, and then paraffin blocked. Slides were made using paraffin blocks and staining was done with haematoxylin-eosin pigments. A microscope was used to examine the skin samples in order to characterise the epidermal and dermal alterations

as well as the signs of inflammation (Qushawy *et al.*, 2018). Figure 2.3 shows complete experimental design.

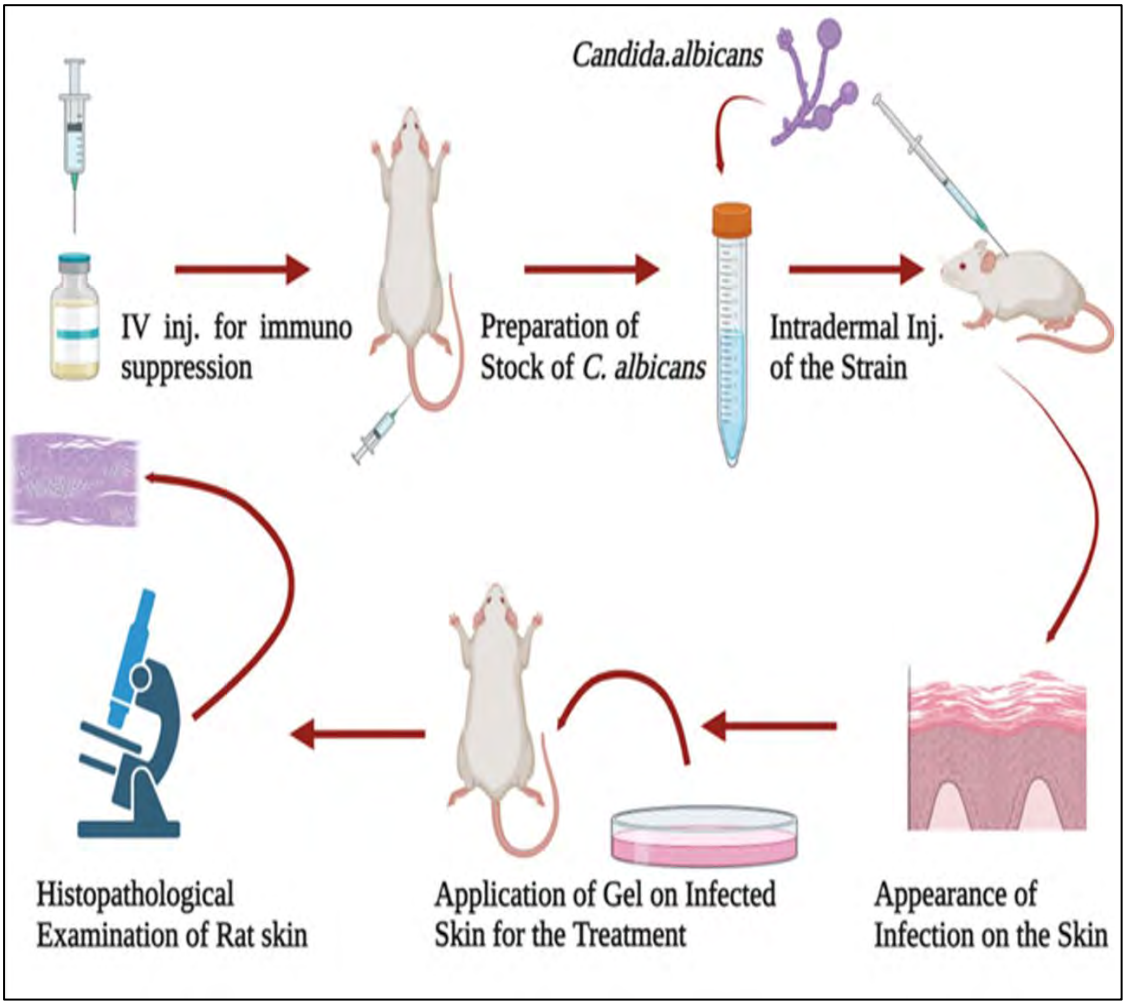

Figure 2.3. Schematic representation of *in vivo* antifungal model (created via Bio render).

2.15. Stability Studies

Stability studies were performed for six months for MCZN TESs and MCZN TESs Gel. Formulation was stored at 25 ± 2° C and 4 ± 2° C. Physical stability, PS, ZP, PDI and EE were observed over the period of six months for MCZN TESs, while physical stability, drug content and pH were monitored for MCZN TESs Gel for six months (Batool *et al.*, 2021).

2.16. Statistical Analysis

The data was expressed as mean standard deviation for all the experiments, which were conducted in triplicate (n=3). The data were statistically analysed using One way Anova and Dunnett's t-test for comparison. Additionally, the Kruskal-Wallis and Mann-Whitney tests were used to determine how the mean values of the two groups

differed from one another. SPSS for Windows (Release 21.0, SPSS Inc., USA) was used to find significant differences between the values. At $p < 0.05$, the P value was reported as significantly different (Batool *et al.*, 2021).

CHAPTER 3

RESULTS

3. RESULTS

3.1. Preparation of Standard Calibration Curve

3.1.1. Standard calibration curve of MCZN

By dilutions from the stock solutions, a standard calibration curve for MCZN was created. Absorbance measurements were recorded after each sample was examined in a UV-spectrophotometer at 272 nm. A calibration curve of MCZN was created after plotting the data on the excel sheet. **Table 3.1** shows the data of Conc. and absorbance used for plotting the graph. Standard calibration curve is shown in **Figure 3.1.**

Table 3.1. MCZN standard calibration curve.

S. No	Conc. (µg/ml)	Absorbance
1	0.625	0.13
2	1.25	0.218
3	2.5	0.39
4	5	0.701
5	10	1.3
6	20	2.51

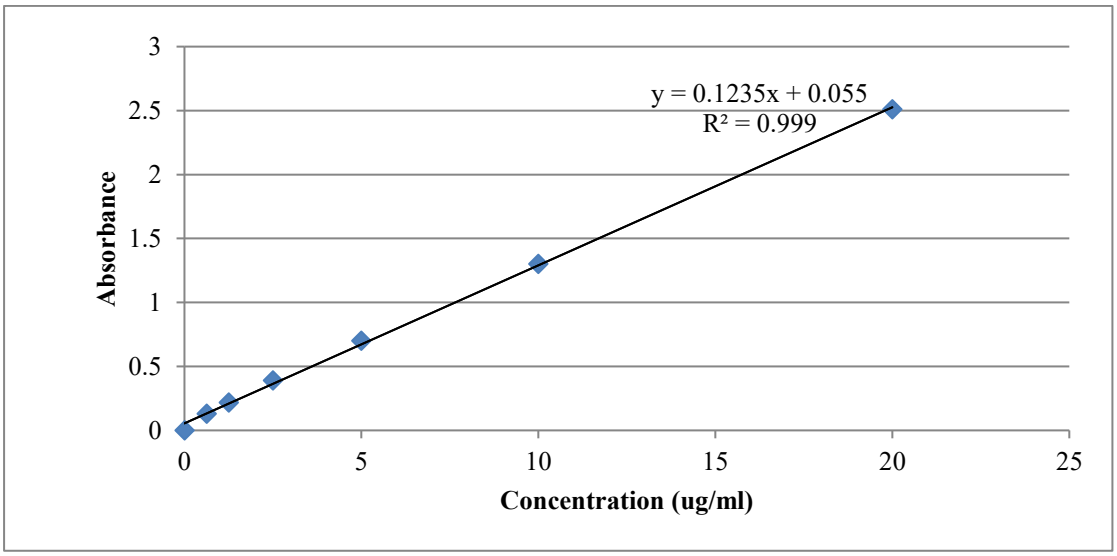

Figure 3.1. Standard calibration curve of MCZN.

3.1.2. Calibration curve of MCZN in PBS pH 7.4

Several dilutions of MCZN were made in phosphate buffer pH 7.4 and all the dilutions were analysed using UV spectrophotometer at wavelength of 272 nm. **Table 3.2** shows the data of Conc. and absorbance used for plotting the graph. Standard calibration curve is shown in **Figure 3.2.**

Table 3.2. Standard calibration curve in PBS pH 7.4.

S. No	Conc. (µg/ml)	Absorbance
1	1.25	0.11
2	2.5	0.219
3	5	0.317
4	10	0.59
5	20	1.13
6	40	2.19

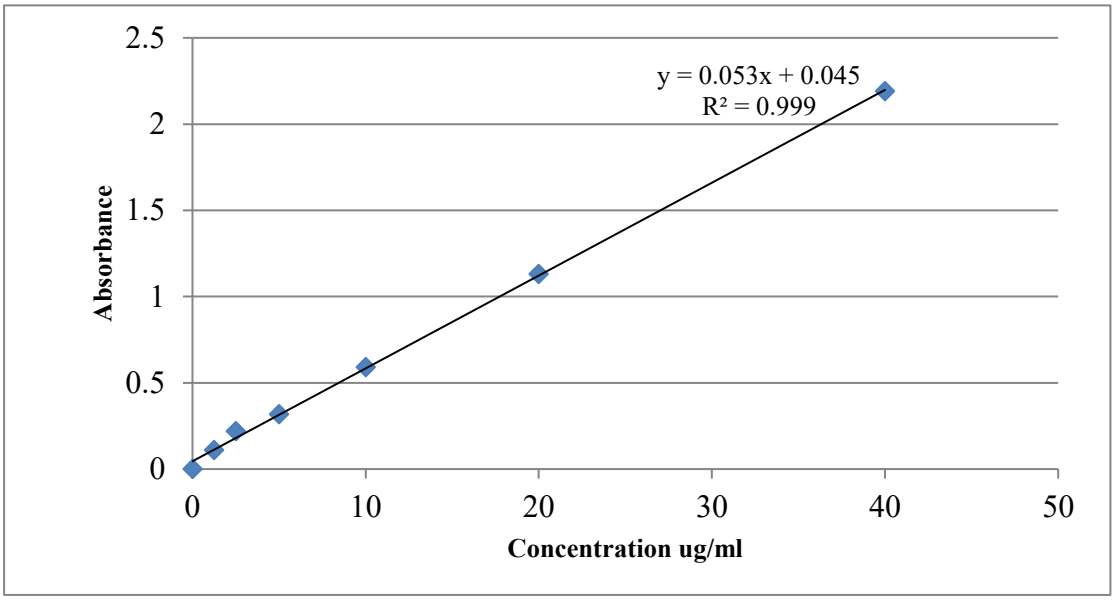

Figure 3.2. Standard calibration curve in PBS pH 7.4.

3.1.3. Calibration curve of MCZN in PBS pH 5.5

Different dilutions were made from stock solution and all the dilutions were analysed at wavelength of 272 nm. **Table 3.3** shows the data of Conc. and absorbance used for plotting the graph. Standard calibration curve is shown in **Figure 3.2.**

Table 3.3. Standard calibration curve in PBS pH 5.5.

S. No	Conc. (µg/ml)	Absorbance
1	0.3125	0.048
2	0.625	0.091
3	1.25	0.149
4	2.5	0.277
5	5	0.511
6	10	0.998

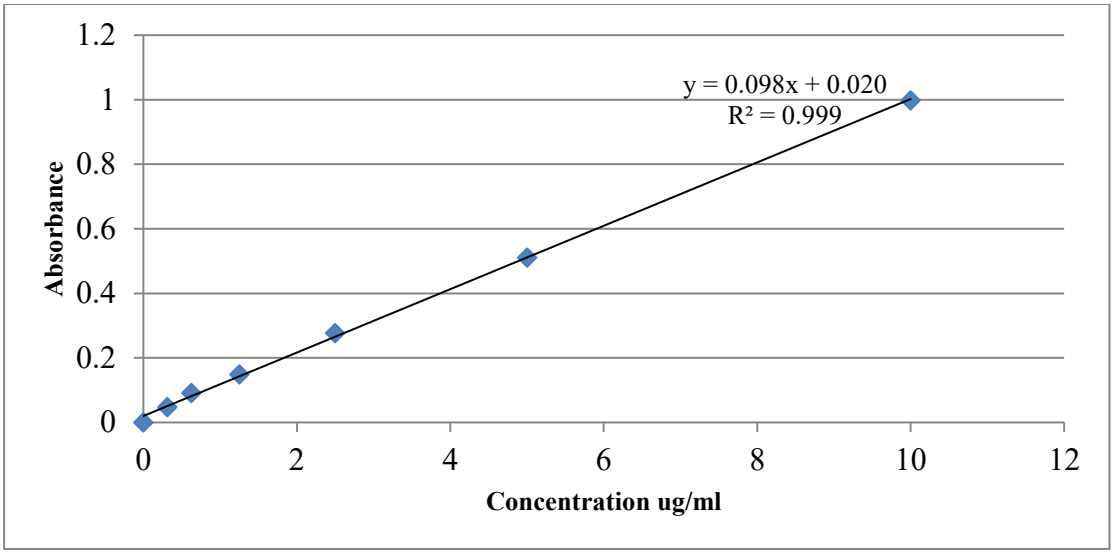

Figure 3.3. Standard calibration curve in PBS pH 5.5.

3.2. Optimization of Blank TESs

TESs were prepared via thin film hydration method. The formulation was milky white in colour. Optimization was done based on three factors that were PDI, ZP and size of the particles formulated. It was observed that by increasing the conc. of lipid from 75 mg to 95 mg and by decreasing surfactant conc. from 15 mg to 5 mg PS was increased from 145 nm to 183.3 nm along with increase in PDI from 0.121 to 0.258 and ZP was increased from -16 mV to -23 mV.

Table 3.4. Optimization of blank TESs.

Formulation code	Lipid (mg)	Surfactant (mg)	PS (nm)	ZP (mV)	PDI
M 1	75	15	145.3 ± 2.8	-16 ± 4.01	0.121 ± 0.005
M 2	80	20	150 ± 3.7	-15 ± 3.22	0.233 ± 0.002
M 3	85	15	158.9 ± 1.9	-17 ± 2.8	0.236 ± 0.031
M 4	90	10	179.9 ± 2.5	-20 ± 5.09	0.241 ± 0.014
M 5	95	5	183.3 ± 4.3	- 23 ± 3.14	0.258 ± 0.027

3.4. Optimization of MCZN TESs by Box- Behnken Design Model

After pre optimization drug loaded TESs were prepared all the experimental runs given by Design® Expert were performed as shown in **Figure 3.4** data of all formulation is given in **Table 3.5**. Run no 6 was given by software as optimized formulation. That showed that optimized formulation of MCZN TESs had the PS of 224.8 ± 5.1 nm, ZP 21.1 ± 1.10 mV, PDI 0.207 ± 0.009 and EE 93.12 ± 0.101%.

Table 3.5. Optimization table of MCZN TESs.

Runs	PL90G (mg)	S 80 (mg)	MCZN (mg)	PS (nm)	ZP (mV)	PDI	EE%
F-1	**87.5**	**20**	**10**	208.15 ± 8.2	12.5 ± 2.1	0.245 ± 0.0028	91.37 ± 0.123
F-2	**87.5**	**5**	**5**	192.3 ± 5.3	15.5 ± 1.3	0.144 ± 0.0007	84.53 ± 0.098
F-3	**95**	**12.5**	**5**	243.7 ± 9.8	7.29 ± 1.6	0.198 ± 0.0424	78.7 ± 0.126
F-4	**95**	**20**	**7.5**	221.5 ± 0.2	7.44 ± 1.1	0.157 ± 0.0106	90.63 ± 0.08
F-5	**80**	**12.5**	**5**	183.2 ± 5.4	9.37 ± 1.9	0.151 ± 0.0102	73.47 ± 0.11
F-6	**87.5**	**12.5**	**7.5**	**224.8 ± 5.1**	**21.1 ± 1.10**	**0.207 ± 0.009**	**93.12 ± 0.101**
F-7	**95**	**5**	**7.5**	289.7 ± 2.61	12.85 ± 1.8	0.44 ± 0.0156	92.17 ± 0.07
F-8	**87.5**	**5**	**10**	280.05 ± 3.6	30.8 ± 1.1	0.366 ± 0.0290	94.52 ± 0.008
F-9	**80**	**20**	**7.5**	164.9 ± 1.83	14.48 ± 1.5	0.124 ± 0.0120	85.21 ± 0.12
F-10	**80**	**5**	**7.5**	186.2 ± 4.1	23.45 ± 2.3	0.231 ± 0.0081	84.76 ± 0.13
F-11	**95**	**12.5**	**10**	250.6 ± 2.11	20.5 ± 1.5	0.2835 ± 0.029	93.17 ± 0.201
F-12	**87.5**	**20**	**5**	190.6 ± 2.5	9.39 ± 2.2	0.135 ± 0.0226	72.14 ± 0.09
F-13	**80**	**12.5**	**10**	194.8 ± 0.91	24.6 ± 2.3	0.27 ± 0.0106	85.99 ± 0.14

Note: *All values represented here are expressed as mean ± SD (n=3); PL90G = Phospholipon 90 G, S 80 = Span 80, MCZN = Miconazole Nitrate*

Figure 3.4. MCZN formulations given by Design® Expert.

3.5. PS and ZP Analysis of Optimized Formulation Given by Design® Expert

At a wavelength of 635 nm and a scattering angle of 90 degrees, the Zeta Sizer Nano ZS 90 instrument was used to evaluate sample particle size and zeta potential. Each outcome was measured three times. PS and ZP of optimized formulation are shown in **Figure 3.5 and Figure 3.6.** PS and PDI of optimized formulation were 224.8 nm and 0.207 respectively and ZP was 21.1 mV.

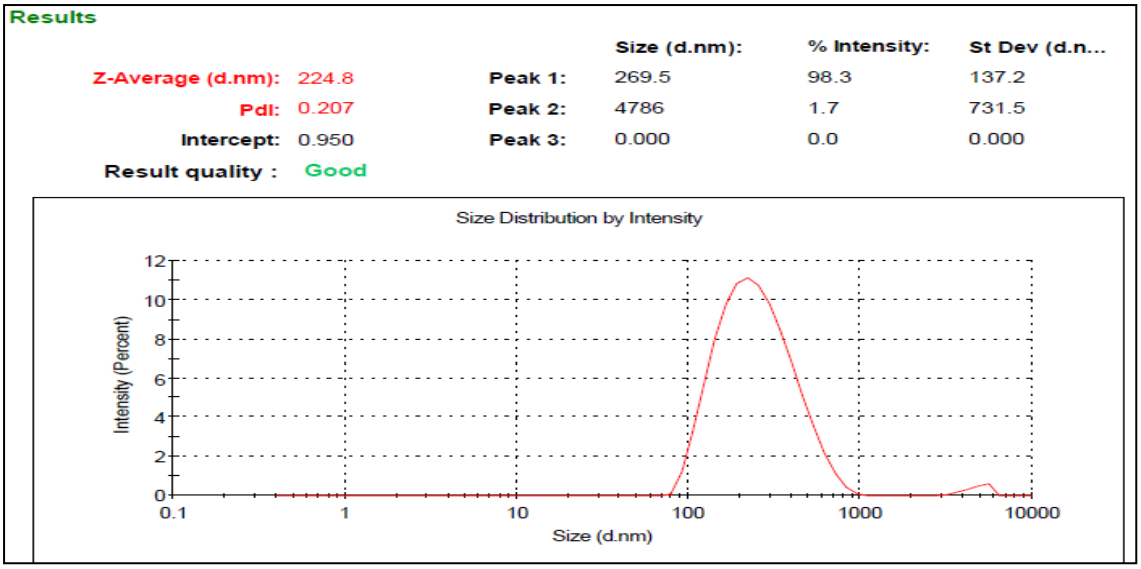

Figure 3.5. PS of optimized formulation.

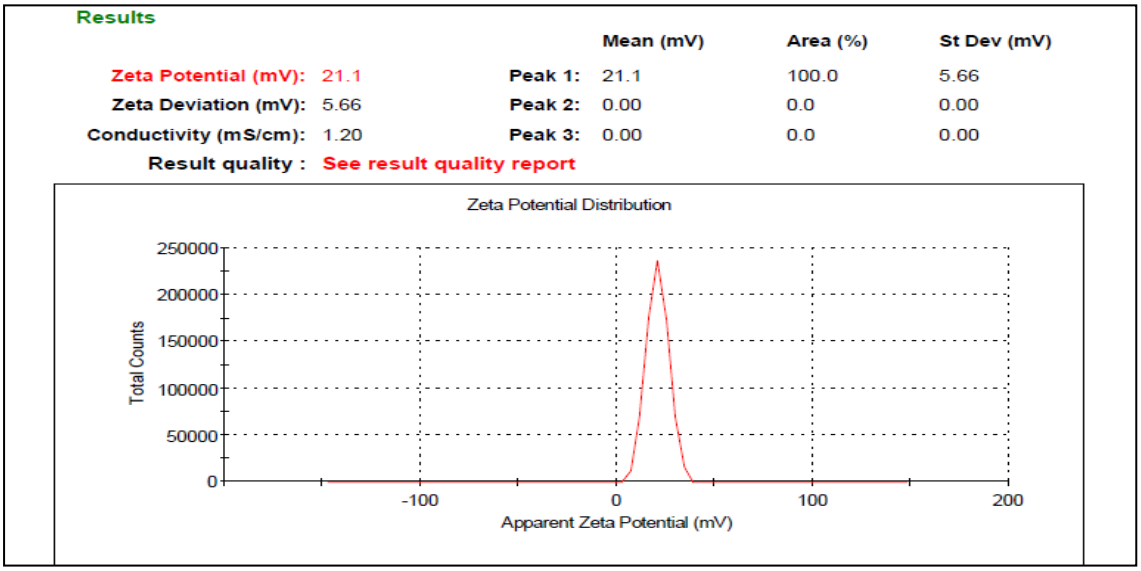

Figure 3.6. ZP of optimized formulation.

3.6. Optimization of MCZN TESs by Box-Behnken Design Model

A two level- three factor Box-Behnken Design employing the software named as Design Expert® (Version 12 Stat-Ease Inc., USA) was used for the optimization of

MCZN TESs. The minimum and maximum level of independent variables and constraints of dependent are shown in **Table 3.6.** Amount of lipid, surfactant and drug were selected as independent variables while PS, ZP, PDI and EE were selected as dependent variables. 13 experimental runs were suggested by Design Expert® and all the runs were performed. The data collected from all the runs showed that particle size of the given runs ranged between 164.9 to 289.75 nm and in the case of zeta potential the 13 experimental runs zeta potential ranged between 7.29 to 30.8 mV. PDI range was 0.124 to 0.44 and entrapment efficiency was from 72.14 to 94.52%.

Table 3.6. Levels of independent variable and constraint of dependent variables.

Variables	Low level (-1)	High level (+1)
Independent Variables		
PL90G (mg)	80	95
S 80 (mg)	5	20
MCZN	5	10
Dependent Variables		
PS (nm)	Maximize	
ZP (mV)	Maximize	
PD1	Minimize	
EE (%)	Maximize	

3.7. Analysis of Data Obtained by Box-Behnken Design

For all the dependent variables that were PS, PDI, ZP and EE regression analysis was performed by the software and the values are given in **Table 3.7.** Best fit model for all the responses was linear model. These values indicate that as ($p < 0.05$) for all the models that were produced by the responses indicating significant results for the models produced. ‘‘Adequate precision’’ was also calculated for each model. The purpose of this adequate precision is measurement of signal to noise ration. And desirable value for this adequate precision should be greater than 4. As all the models showed these values greater than 4 given in **Table 3.7** which means models can navigate the design space. **Table 3.7** also shows that ‘‘predicted R^{2}’’ and ‘‘adjusted R^{2}’’ values have the difference < 0.2 that means they are in reasonable agreement.

Coded equations were also generated by the software for the analysis of magnitude of affect that was produced by the independent variables. These values can be positive and negative indicating synergistic and antagonistic affect respectively of factors on responses.

Particle size: R_1 = +218.28+34.56A-19.64B+14.74C

Zeta potential: R2 = +16.76-2.98A-4.85B+5.86C

PDI: R_3 = +0.2171+0.0377A-0.0526B+0.0546C

EE: R_4 = +86.67+2.03A-2.45B+6.78C

In the above equations R is the indication of response. A represents PL90G, B represents S 80 and C represents MCZN.

Table 3.7. Regression analysis by Design Expert®.

Responses	R^2	Adjusted R^2	Predicted R^2	Adequate Precision
PS	0.8334	0.7879	0.6505	12.9858
ZP	0.7625	0.6977	0.5714	10.6676
PDI	0.6377	0.5389	0.2299	7.6257
EE	0.6752	0.5867	0.4493	8.3573

3.8. Characterization of MCZN TESs

3.8.1. Effect of independent variable on PS

In case of deep-seated fungal infection size of vesicles is very important to cross the skin barriers. All the vesicles showed desirable vesicle size in all the 13 experimental runs. The effect of independent variables on PS has been shown in **Figure 3.7.** PL90G had the significant effect on PS as (p = 0.0001), as with increased concentration from 80 mg to 95 mg while keeping surfactant constant PS was increased from 183.2 ± 5.4 nm (F-5) to 250.6 ± 2.11 nm (F-11) . Similar synergistic effect was seen with MCZN (p = 0.0257) on PS. On contrary by increasing conc. of S 80 (p = 0.0056) from 5 mg to 20 mg PS was significantly reduced from 280.05 ± 3.6 nm (F-8) to 208.15 ± 8.2 nm (F-1) as shown in **Table 3.5.**

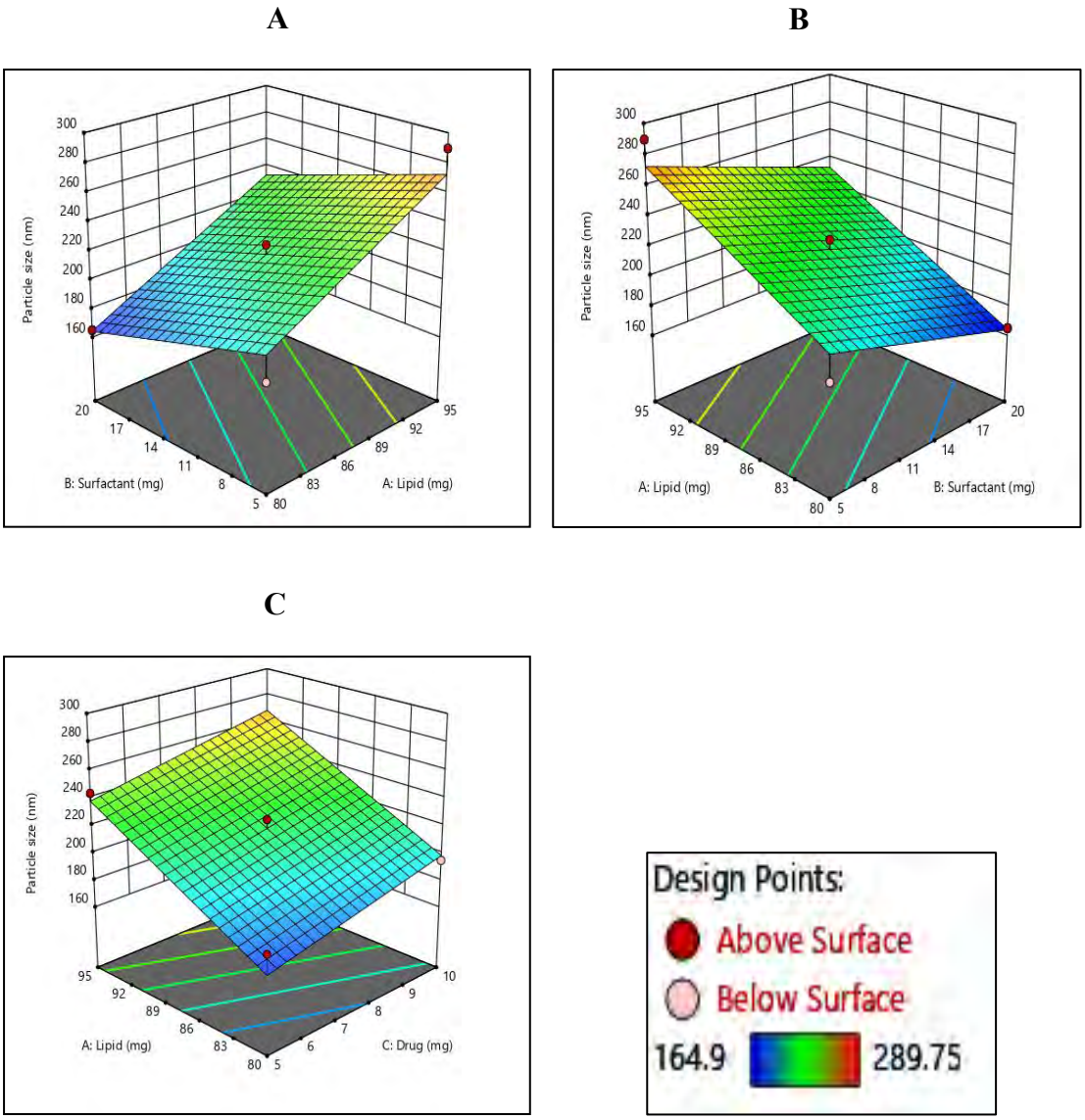

Figure 3.7. Three dimensional graphs showing the effect of independent variables on particle size of MCZN TESs.
***Note:* A:** *effect of lipid and surfactant on PS,* **B:** *effect of surfactant and drug on PS,* **C:** *effect of drug and lipid on PS.*

3.8.2. Effect of independent variable on ZP

The optimised formulation revealed a 21.1 mV zeta value while the minimum and maximum values were 7.29 mV and 30.8 mV respectively. MCZN (p = 0.0013) had the most significant effect on zeta potential. Increase in the concentration of MCZN resulted in increased ZP. For example, when we increased the conc. of drug from 5 mg to 10 mg while keeping PL90G and S 80 constant ZP increased from 15.5 ± 1.3 mV (F-2) to 30.8 ± 1.1 mV (F-8). Moreover, S 80 (p = 0.0047) had cause reduction in ZP when its conc. was increased from 5 mg to 20 mg while keeping drug and lipid constant

ZP was reduced from 30.8 ± 1.1 mV to (F-8) to 12.5 ± 2.1 mV (F-1) as observed from **Table 3.5.**

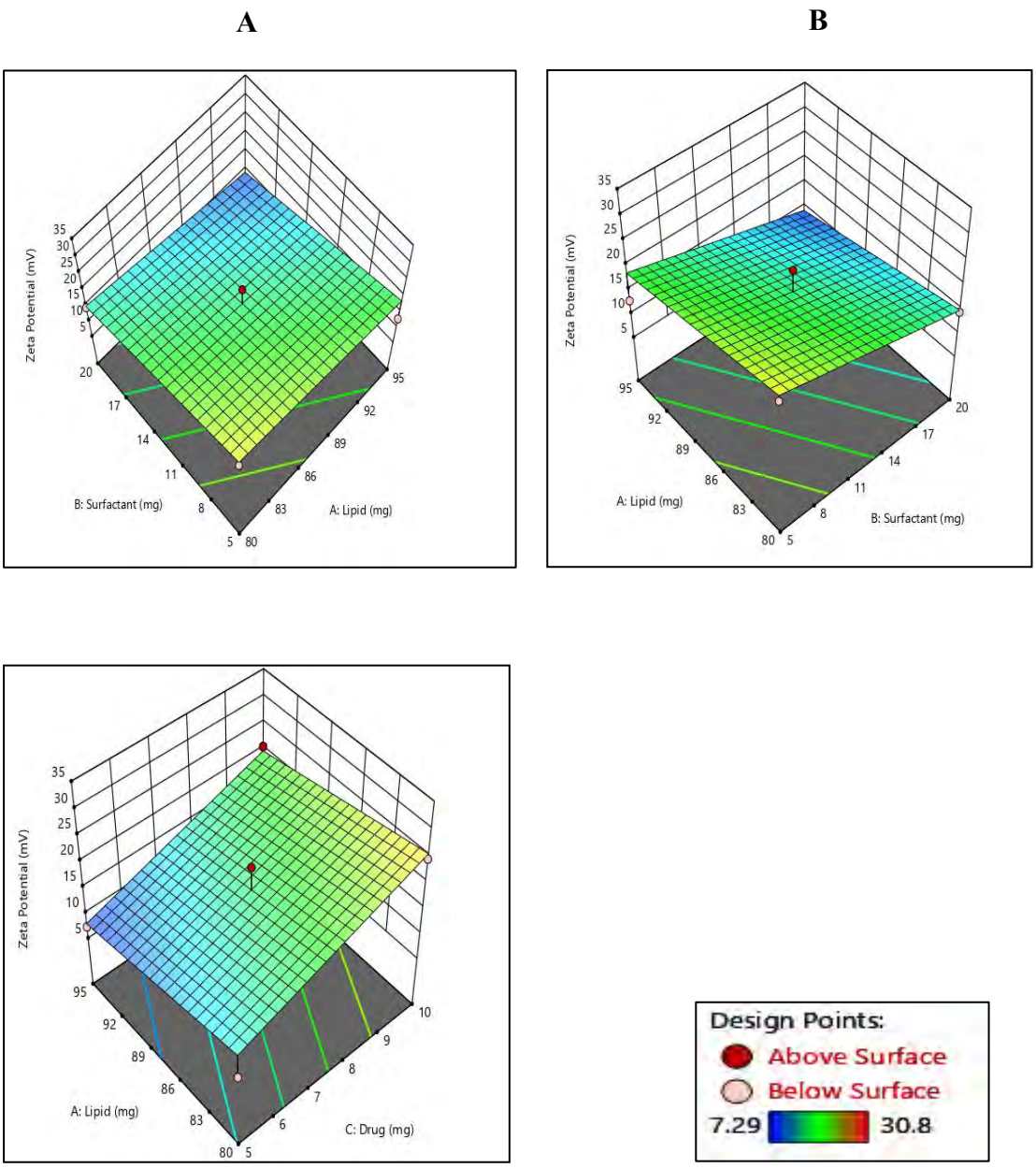

Figure 3.8. Three dimensional graphs showing the effect of independent variables on Zeta potential of MCZN TESs.
Note: A: *effect of lipid and surfactant on ZP,* ***B:*** *effect of surfactant and drug on ZP,* ***C:*** *effect of drug and lipid on ZP.*

3.8.3. Effect of independent variables on PDI

MCZN (p = 0.0162) had positive effect on PDI when its conc. was increased from 5mg to 10 mg while keeping lipid and surfactant constant PDI value was enhanced from 0.144 ± 0.0007 (F-2) to 0.366 ± 0.0290 (F-8). Similarly, PL90G (p = 0.0755) also has synergistic effect on PDI with its increased conc. from 80 mg to 95 mg where drug and

surfactant were kept constant, PDI was increased from 0.27 ± 0.0106 (F-13) to 0.2835 ± 0.029 (F-11). S 80 with (p = 0.0195) has antagonistic effect on PDI, when its conc. was increased from 5 mg to 20 mg while keeping the lipid and drug constant PDI was decreased from 0.44 ± 0.0156 (F-7) to 0.157 ± 0.0106 (F-4) as shown in **Table 3.5.** The range of PDI values for all the produced formulations is shown in **Figure 3.6.**

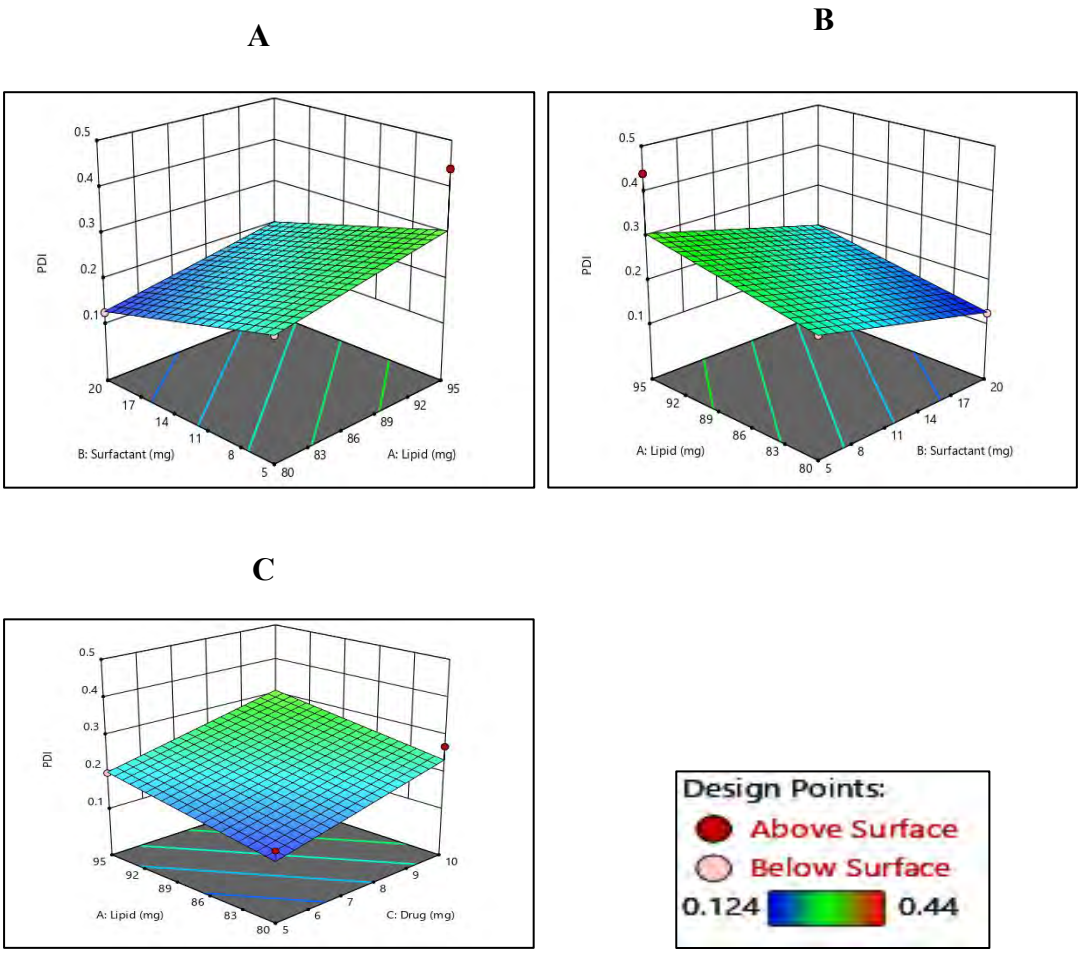

Figure 3.9. Three dimensional graphs showing the effect of independent variables on poly dispersity index of MCZN TESs.
Note: A: *effect of lipid and surfactant on PDI,* ***B:*** *effect of surfactant and drug on PDI,* ***C:*** *effect of drug and lipid on PDI.*

3.8.4. Effect of independent variables on EE

Minimum and maximum values for EE were 72.14% and 94.52%. MCZN (p = 0.015) had the positive effect on entrapment, when its conc. was increased from 5 mg to 10 mg while keeping lipid and surfactant constant, EE was increased from 78.7% ± 0.126 (F-3) to 93.17% ± 0.201 (F-11)**.** When PL90G (p = 0.0852) conc. was increased from 80 mg to 95 mg where drug and surfactant were kept constant, EE was increased from 85.99% ± 0.14 (F-13) to 93.17% ± 0.201 (F-11) as shown in **Table 3.5.**

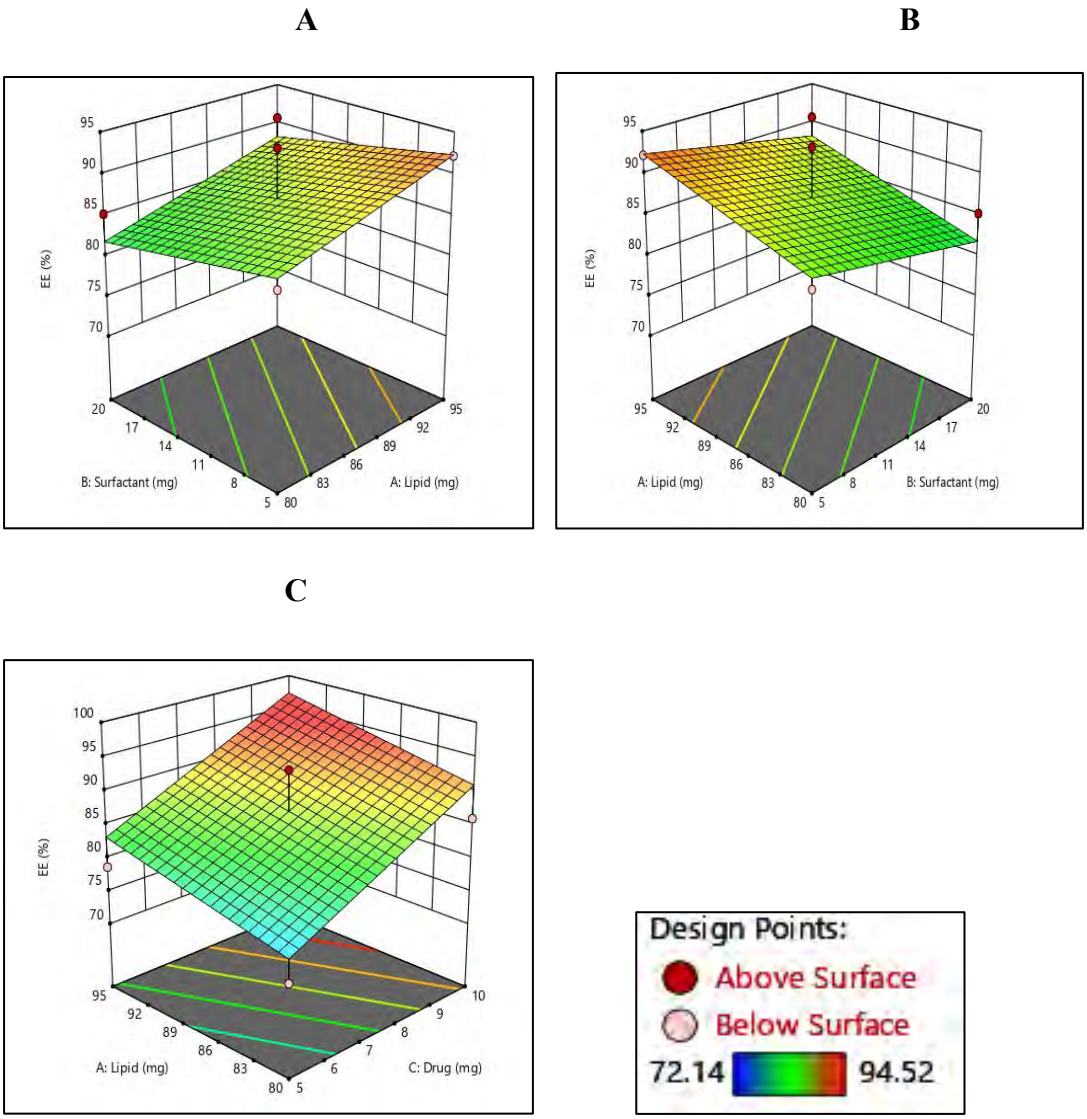

Figure 3.10. Three dimensional graphs showing the effect of independent variables on entrapment efficiency of MCZN TESs.
Note: A: *effect of lipid and surfactant on EE,* ***B:*** *effect of surfactant and drug on EE,* ***C:*** *effect of drug and lipid on EE.*

3.8.5. FTIR analysis report of MCZN TESs

The analysis was carried out from 4000 cm^{-1} to 400 cm^{-1}. MCZN showed major peaks at 1381 cm^{-1}, 3107 $cm^{-1}$and 2963 cm^{-1} showing imidazole groups C-N stretch, aromatic stretching at C-H, and aliphatic C-H stretching respectively. Other major peaks of MCZN were 1507cm^{-1} that shows aromatic-C-C- bonding, 1474 cm^{-1} shows $–CH_2$ bending, 1328 cm^{-1} –C-N- stretching, -C-O- stretch was shown at peak 1170 cm^{-1}, aromatic out of plane bend was shown at peak 827 cm^{-1} and 637 cm^{-1} shows-C-CL- stretch. The analysis findings showed that there was no interaction between the MCZN,

the MCZN TESs, and PL90G and physical mixture (PM). In the final formulation peak, both drug and lipid peaks were preserved; no additional peaks were seen.

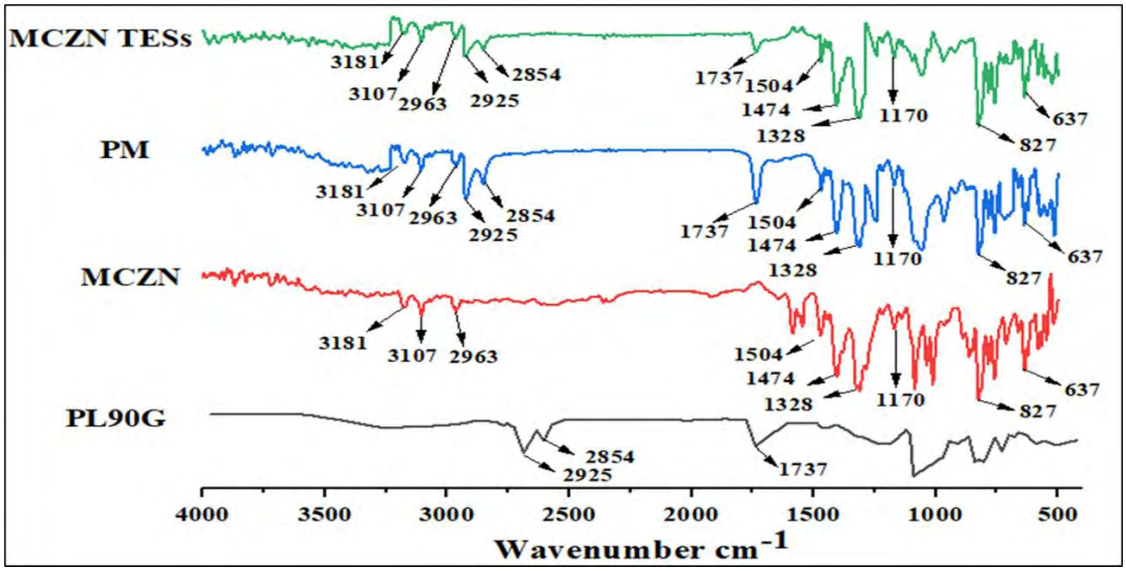

Figure 3.11. FTIR analysis report of MCZN and its components carried at 4000 to 400 cm^{-1}.

3.8.6.DSC analysis report

DSC analysis was carried out for MCZN TESs, MCZN and PL90G. **Figure 3.12** shows that MCZN showed a large endothermic peak at the temperature of 186.485 °C but this peak disappeared in the final formulation that was MCZN TESs.

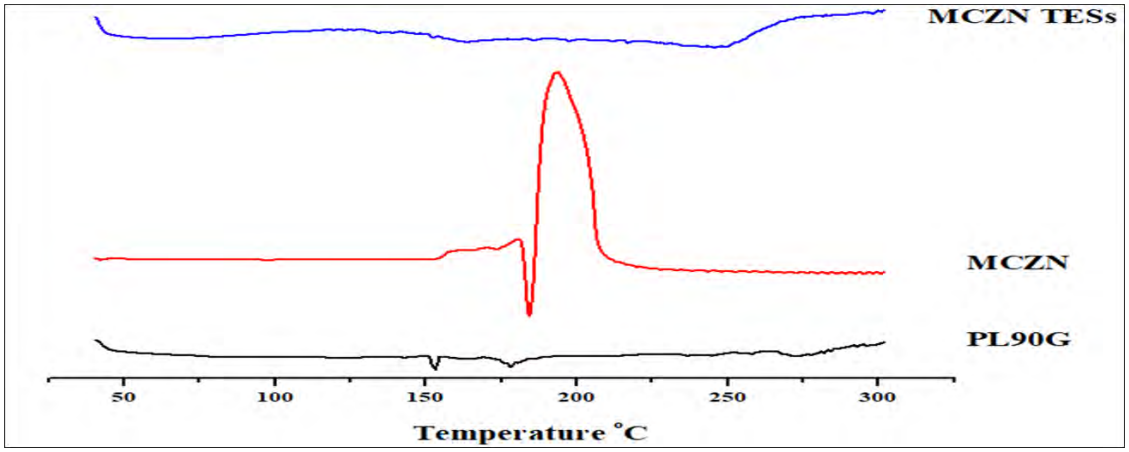

Figure 3.12. DSC analysis of MCZN.

3.8.7. DI and elasticity study of MCZN TESs vesicles

DI is a measurement of the ability to change shape in response to the environment. Values near 1 represent the particles possess a strong ability to adapt in challenging circumstances. Before and after extrusion values were 224.8 ± 5.1 nm and 211 ± 4.9 nm. So, DI was 0.94 and %DI was 94.196%. elasticity was 2.11 ± 0.02, proving that

optimized formulation of MCZN TESs was deformable as well as elastic (Rabia *et al.*, 2020).

3.9. Preparation of MCZN TESS Gel

Chitosan gel with different concentrations was prepared and evaluated on the bases of its physiochemical characteristics. Gel prepared with 2% concentration was considered optimized and further evaluated.

Figure 3.13. MCZN TESs Gel.

3.10. Characterization of MCZN TESs Gel

3.10.1. Spreadability

Glass slide method was employed for spreadability determination. Spreadability of gel was 333.712 ± 9.21%. Which indicated that gel spreadability was in ideal range.

A **B**

Figure 3.14. A and **B** shows spreadability of MCZN TESs gel via glass slide method.

3.10.2. Rheological study

The deformability of a material under the influence of an applied force is demonstrated through rheology. Liquids typically exhibit non-Newtonian behaviour, or viscosity that depends on stress. When the shear rate of a gel was tested at various levels, it was found that viscosity decreased as shear rate increased and was increased as shear rate was decreased as it can be seen from **Figure 3.15**. In this instance, the viscosity and applied stress showed an inverse relationship, and the gel flowed in a pseudoplastic or non-

Newtonian manner. Shear thickening gels are those sorts of gels whose viscosity and applied stress are directly correlated.

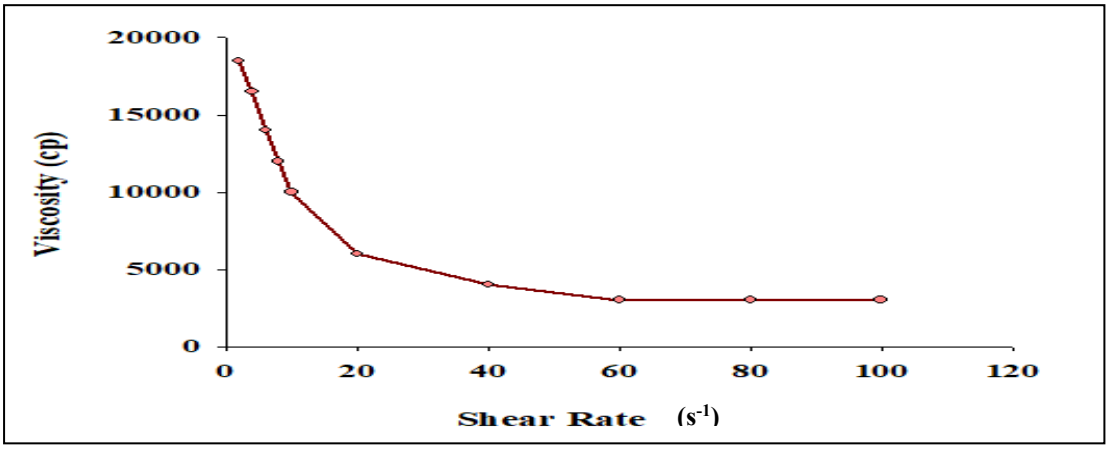

Figure 3.15. Flow behaviour of MCZN TESs gel.

3.10.3. pH of gel

pH of MCZN TESs gel was measured in triplicate and it was 5.7 ± 0.3. This value is considered in ideal range for topical formulations.

3.10.4. Clarity, Homogeneity and Drug Content

The prepared gel was milky white in colour and was homogeneous without any particles or impurities. Drug content of gel was 98.87 ± 1.03%.

3.11. *In Vitro* Release Study at pH 5.5

Mechanical shaker bath was used to perform release studies at pH 5.5. The release studies showed that MCZN dispersion gave the release 100% within 6 hours. MCZN Gel and Marketed Gel gave release of 100% and 97.5% respectively within 8 hours. MCZN TESs gave prolong release of 88.043% in 24 hours. MCZN TESs Gel gave release of 76.1164% within 24 hours. As it can be clearly observed from **Figure 3.16.**

3.12. Kinetics of Drug Release for MCZN TESs and MCZN TESs Gel

All kinetic models were applied on MCZN TESs and MCZN TESs Gel. R^2 value was highest in Krosmeyer-peppas model as shown in **Table 3.8** in case of MCZN TESs with n=0.306 showing fickian diffusion. In case of MCZN TESs Gel R^2 value was highest for Higuchi model and release type was non-fickian diffusion.

Table 3.8: Kinetic modelling of MCZN TESs and MCZN TESs Gel.

Formulations	Zero Order	First Order	Hixson Crowell	Higuchi	Krosmeyer-Peppas	
	R^2	R^2	R^2	R^2	R^2	n
MCZN TESs	-0.2397	0.8938	0.8037	0.7938	**0.9574**	**0.306**
MCZN TESs Gel	0.5835	0.9472	0.8987	**0.9774**	0.9561	**0.479**

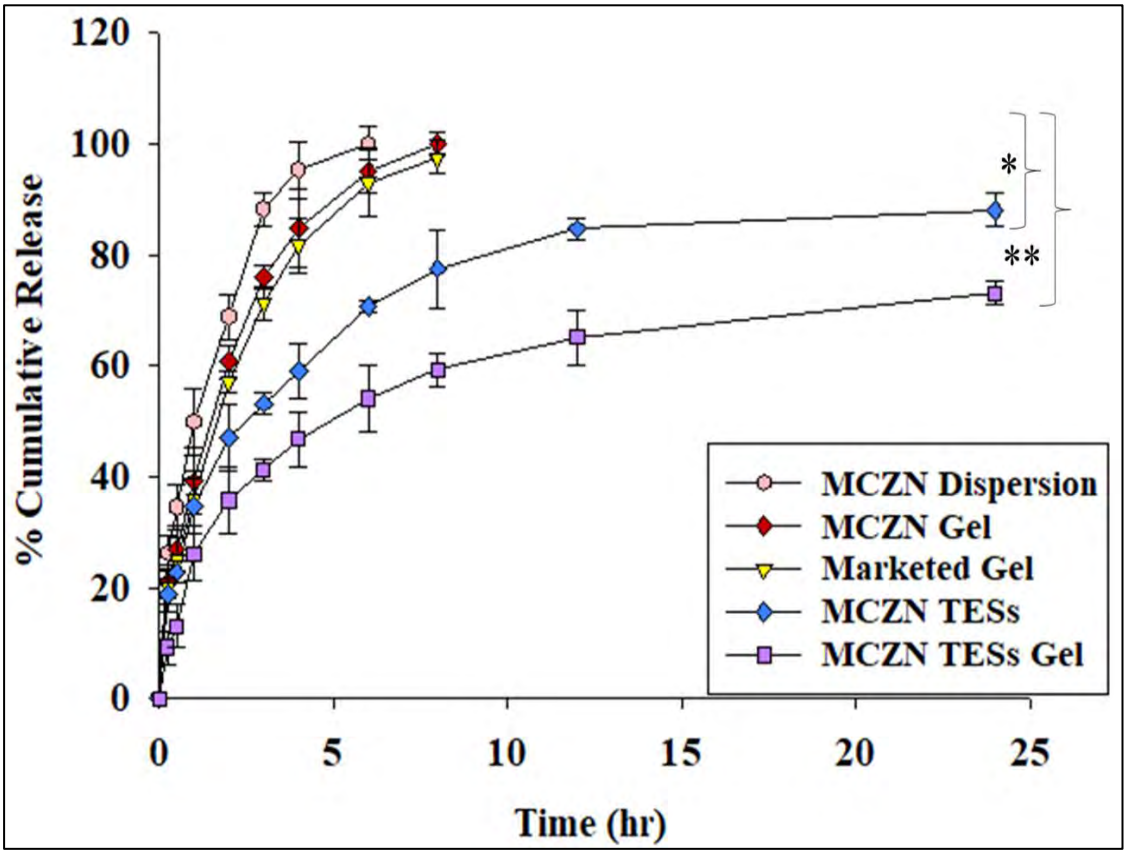

Figure3.16. *In Vitro* Release of MCZN at pH 5.5.
Note: *(*P < 0.05) In vitro Release of MCZN TESs compared with MCZN Dispersion;) (**P < 0.01) In vitro Release of MCZN TESs Gel compared with MCZN Dispersion. Data expressed as mean ± S.D (n=3).*

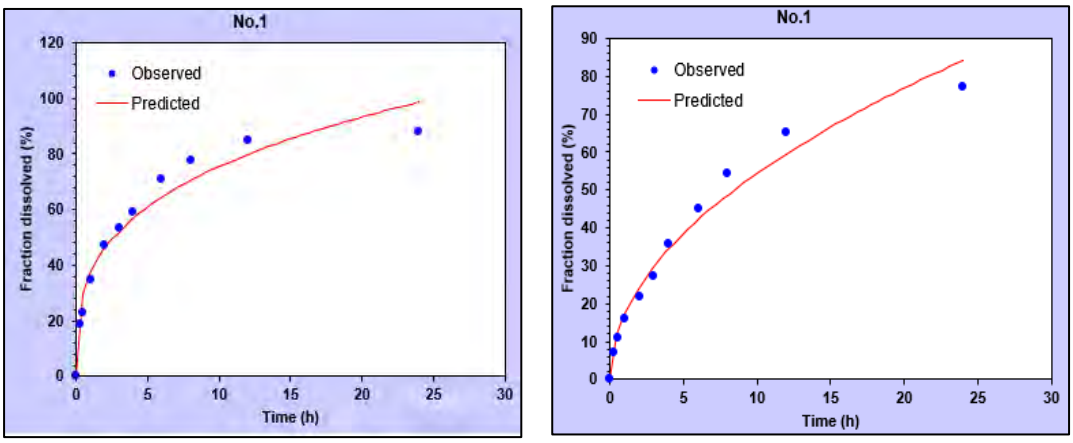

A **B**

Figure 3.17. A: Difference between observed and predicted in Krosmeyer-Peppas Model of MCZN TESs **B:** Difference between observed and predicted in Higuchi Model of MCZN TESs Gel.

3.13. Ex Vivo Permeation and Deposition Study

Ex vivo skin permeation study was performed for MCZN TESs, MCZN TESs Gel, Marketed Gel and MCZN Gel using Franz diffusion cell apparatus. After 24 hours total amount of drug permeated in case of MCZN TESs, MCZN TESs Gel, Marketed Gel and MCZN Gel was 369.6406 µg/cm^2, 254.1406 µg/cm^2, 77.8210 µg/cm^2 and 73.2112 µg/cm^2.As shown in **Figure 3.18.**

After 24 hours skin was removed from the Franz diffusion apparatus and deposition studies were performed as shown in **Figure 3.19** which shows that in case of MCZN TESs Gel maximum amount of drug was retained in epidermis/dermis i.e., 50.87%. in case of MCZN TESs 28% of drug was retained in epidermis/dermis. This shows that TESs has the capability of penetrating into deeper layer of skin for local therapeutic action as compared to Marketed Gel and MCZN Gel in which deposition of drug was only 13.1% and 12.21% respectively. **Table 3.9** shows permeation flux and enhancement ratio calculated for MCZN TESs, MCZN TESs Gel, Marketed Gel and MCZN Gel.

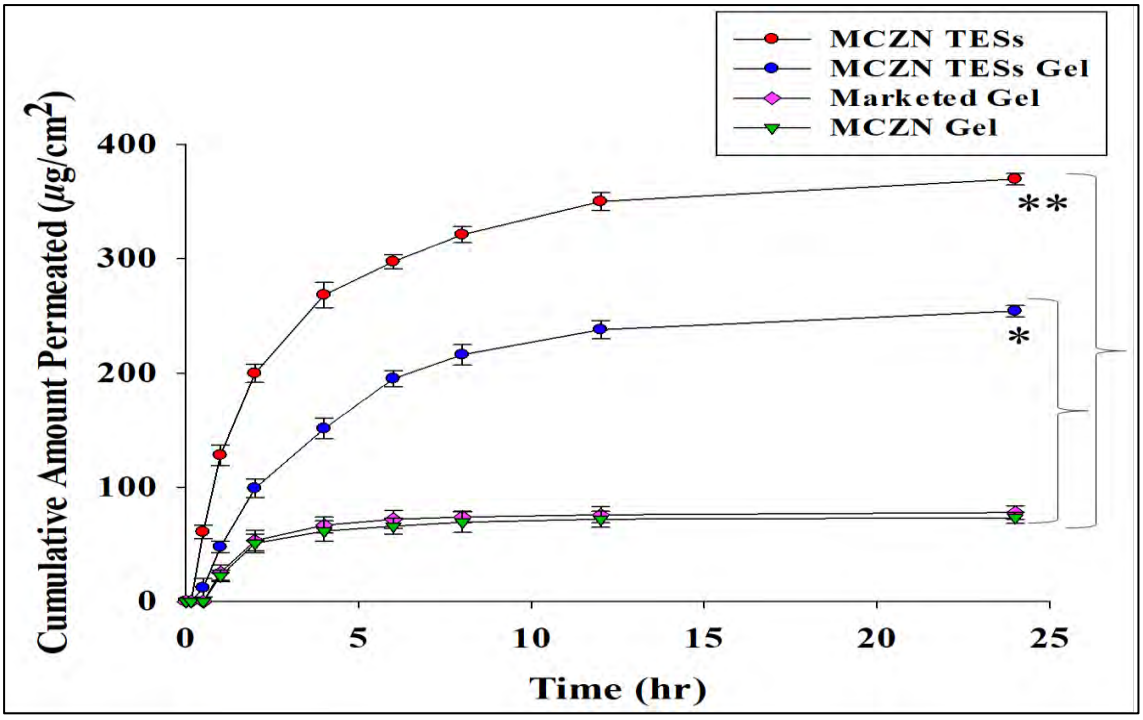

Figure 3.18. Ex vivo skin permeation of MCZN formulations.
Note: *(** p< 0.01) Ex Vivo Permeation of MCZN TESs compared with MCZN Gel and Marketed Gel; (* p< 0.05) Ex vivo permeation of MCZN TESs Gel compared with MCZN Gel and Marketed Gel; Data expressed as mean ± S.D.*

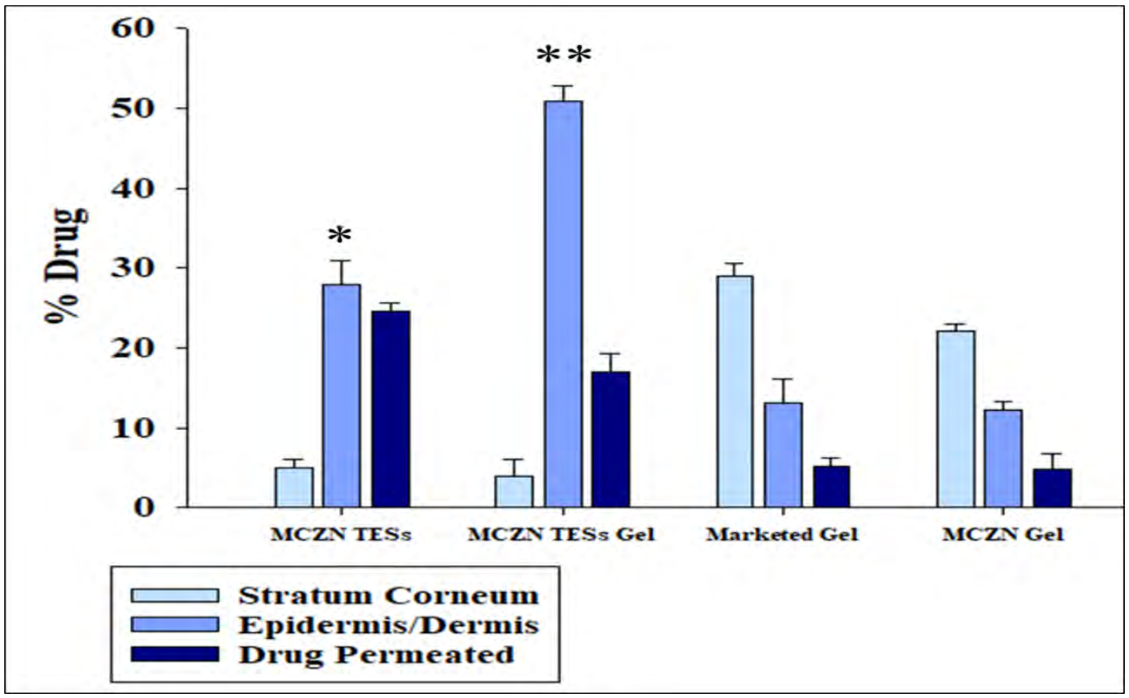

Figure 3.19. Skin deposition study of MCZN formulations.
Note: *(**p < 0.01) MCZN TESs Gel compared with Marketed Gel and MCZN Gel; (*p < 0.05) MCZN TESs compared with Marketed Gel and MCZN Gel, Data expressed as mean ± S.D (n=3).*

Table 3.9. Permeation profile of Miconazole Nitrate formulations.

Formulations	Total Drug Amount Permeated in 24 hrs Q (ug/cm²)	Flux Jss (ug/cm²/h)	Enhancement Ratio
MCZN TESs	369.64 ± 3.88	15.401	5.049
MCZN TESs Gel	254.14 ± 1.61	10.589	3.471
Marketed Gel	77.8210 ± 1.16	3.2425	1.06
MCZN Gel	73.211± 1.084	3.05	1

Note: *Each value represents the mean ± SD (n=3). MCZN TESs= Miconazole Nitrate transethosomes; MCZN TESs Gel= Miconazole Nitrate transethosomal gel; MCZN Gel= Miconazole Nitrate* gel

3.14: Skin Irritation Studies of MCZN Formulations

Figure 3.20: Skin irritation testing was done to verify the prepared MCZN TESs Gel safety and non-irritancy. Blue arrow in **Figure 3.20 C** shows redness and irritation caused by formalin. There were no sign of edema and erythema on MCZN TESs treated skin as it can be clearly seen in **Figure 3.20 B**. Draize scoring test was performed as shown in **Table 3.10.** PDII for formalin treated skin was 3.75 as compared to MCZN TESs gel treated group which was 1.

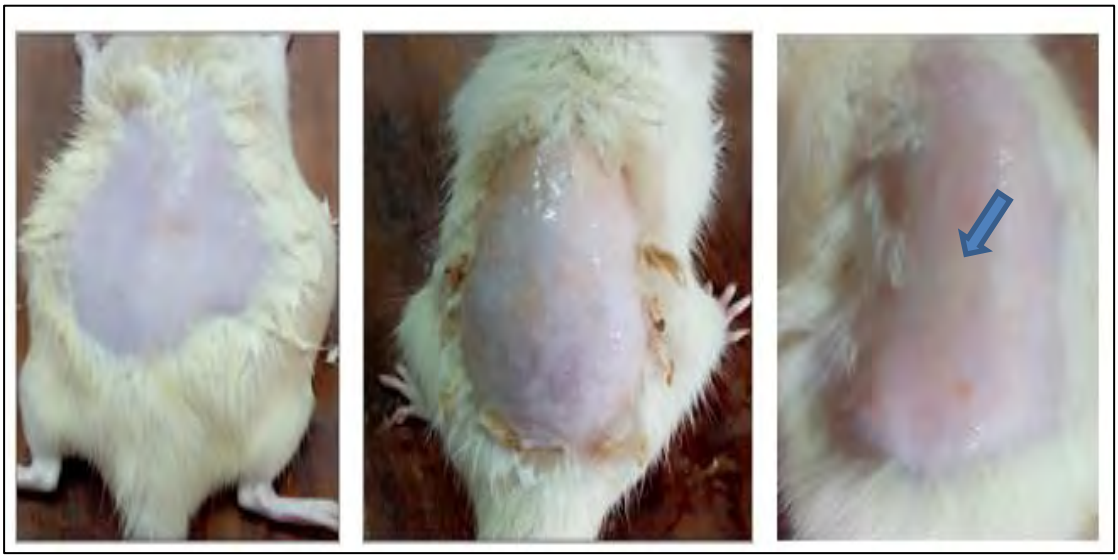

A **B** **C**

Figure 3.20. Skin irritation studies on rats' skin.
Note: A: *Normal skin;* ***B:*** *MCZN TESs Gel treated;* ***C:*** *Formalin treated*

Table 3.10. Skin irritancy scoring.

S.NO	Groups	Time (h)	Edema	Erythema	PDII
1	**Untreated**	0	0	0	**0**
		24	0	0	
		48	0	0	
		72	0	0	
			Total edema score= 0	Total erythema score= 0	
2	**0.8% Formalin Treated**	0	0	0	**3.75**
		24	2	3	
		48	3	3	
		72	2	2	
			Total edema score = 1.75	Total erythema score = 2	
3	**MCZN TESs Gel Treated**	0	0	0	**1**
		24	0.5	0.5	
		48	0	0	
		72	0	0	
			Total edema score = 0.5	Total erythema score = 0.5	

Note: *PDII = Primary dermal irritancy index.*

3.14.1. Skin FTIR analysis

Skin FTIR analysis was performed to check if there of any kind of changes in skin structure when the MCZN TESs Gel is applied. **Figure 3.21** shows that all the peaks present in O-H stretching, lipid C-H stretching and protein C-N stretching region of normal skin were also present in MCZN TESs Gel treated skin indicating no major changes in skin structure.

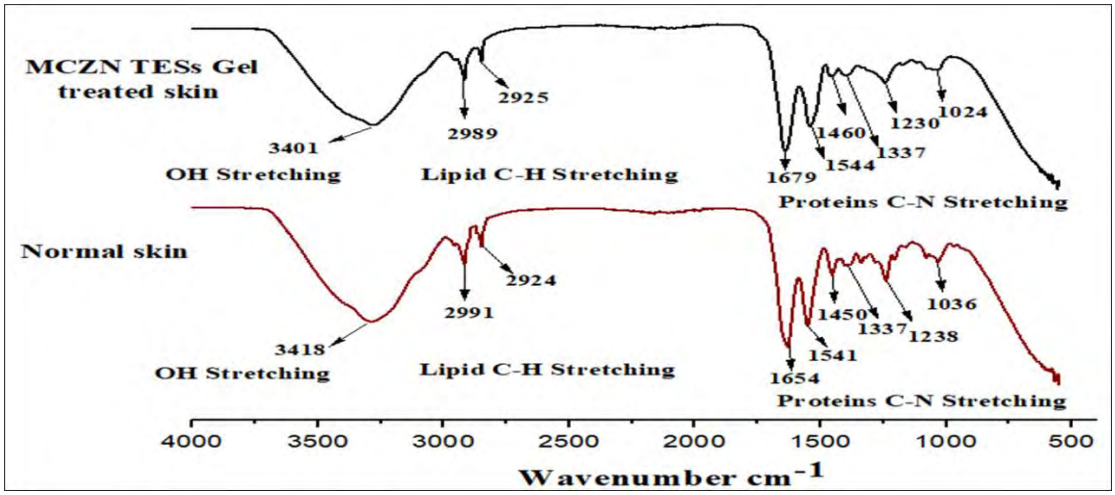

Figure 3.21. FTIR analysis of normal skin and MCZN TESs Gel treated skin.

3.15. Antifungal Assay of Miconazole Nitrate Formulations

Antifungal activity of prepared MCZN TESs Gel was compared to Marketed Gel (Daktarin) and MCZN Gel against *C. albicans* via agar well diffusion method as shown in **Figure 3.22**. Antifungal activity assessment was done based on diameter of zone of inhibition. **Figure 3.23** shows that MCZN TESs gel zone of inhibition was 43 mm much greater as compared to Marketed Gel and MCZN Gel having ZOI of 23 mm and 18 mm respectively measure after 48 hours.

Figure 3.22. Zone of Inhibitions of Miconazole Nitrate Formulations.
***Note:* C. A** = *Candida Albicans*; **T**= *MCZN TESs Gel*; **M** = *Marketed Gel*; **D** = *Drug Gel*

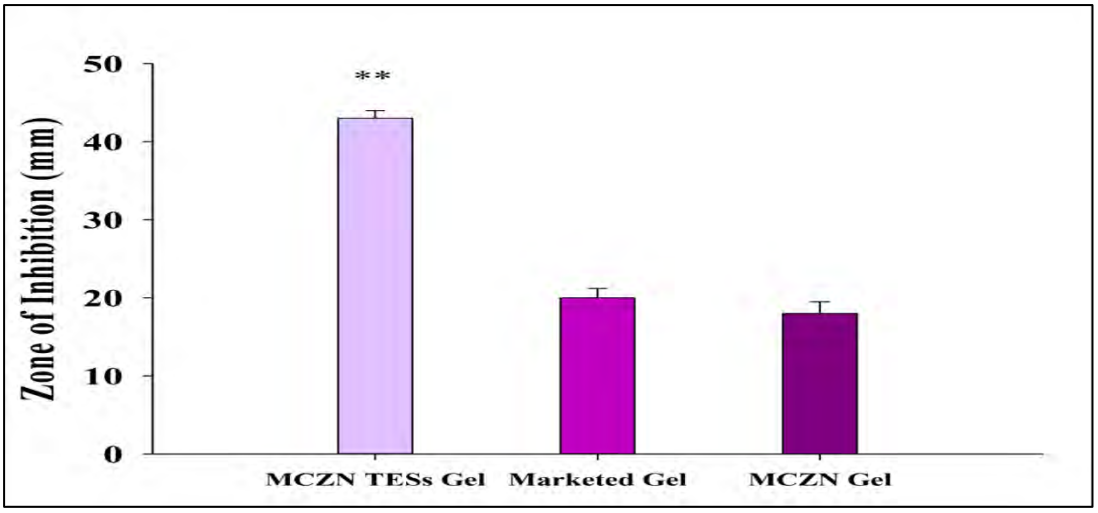

Figure 3.23. Total diameter ZOI in mm measured after 48 hours.
Note: *(**p < 0.01) ZOI of MCZN TESs Gel compared with Marketed Gel and MCZN Gel*
All values are expressed as mean ± S.D (n=3).

3.16. *In Vivo* Antifungal Model for Cutaneous Candidiasis

3.16.1. Evaluation of rat's skin before and after treatment

Before induction with fungal strains all rats' skins were normal having no signs of infection as shown in **Figure 3.24**. At the 7th day all rats' skin fully showed symptoms of infection that are explained in **Table 3.11**. Rashes/colour changes, cracking, scaling, erythema, and inflammation all these symptoms were present on the skin. Positive control group in which no treatment was given infection got worse with the passage of time as it can be clearly seen in **Figure 3.24**. MCZN TESs Gel treated group was healed completely within 7 days. Before and after treatment observation are explained in **Table 3.11** for MCZN TESs Gel treated group. Marketed Gel treated group and MCZN Gel treated group took 10 days for healing. At 10th day slight inflammation was present in Marketed Gel treated group and little scars were left in case of MCZN Gel treated group.

Table 3.11. Effect observed on the skin before and after treatment of MCZN TESs Gel treated group.

Effects Observed	After Induction	After Treatment
Rashes / Colour Changes	+	_
Cracking	+	_
Scaling	+	_
Erythema	+	_
Inflammation	+	_

3.16.2. Histopathological analysis of rat's skin after treatment

Figure 3.25: A is the Histology of positive control group that shows acanthosis marked with red arrow along with mild hyper keratosis marked with blue arrow along with hyphae present in epidermis shown with white arrow. **Figure 3.25: B** shows MCZN TESs Gel treated group with normal epidermis and dermis pointed out with white arrow. **Figure 3.25: C** shows Marketed Gel treated group skin was normal but there was slight inflammation as shown with white arrow. **Figure 3.25: D** shows MCZN Gel treated group having scarred skin marked with white arrow. **Table 3.12.** shows histopathological examination scoring for quantitative evaluation of antifungal activity

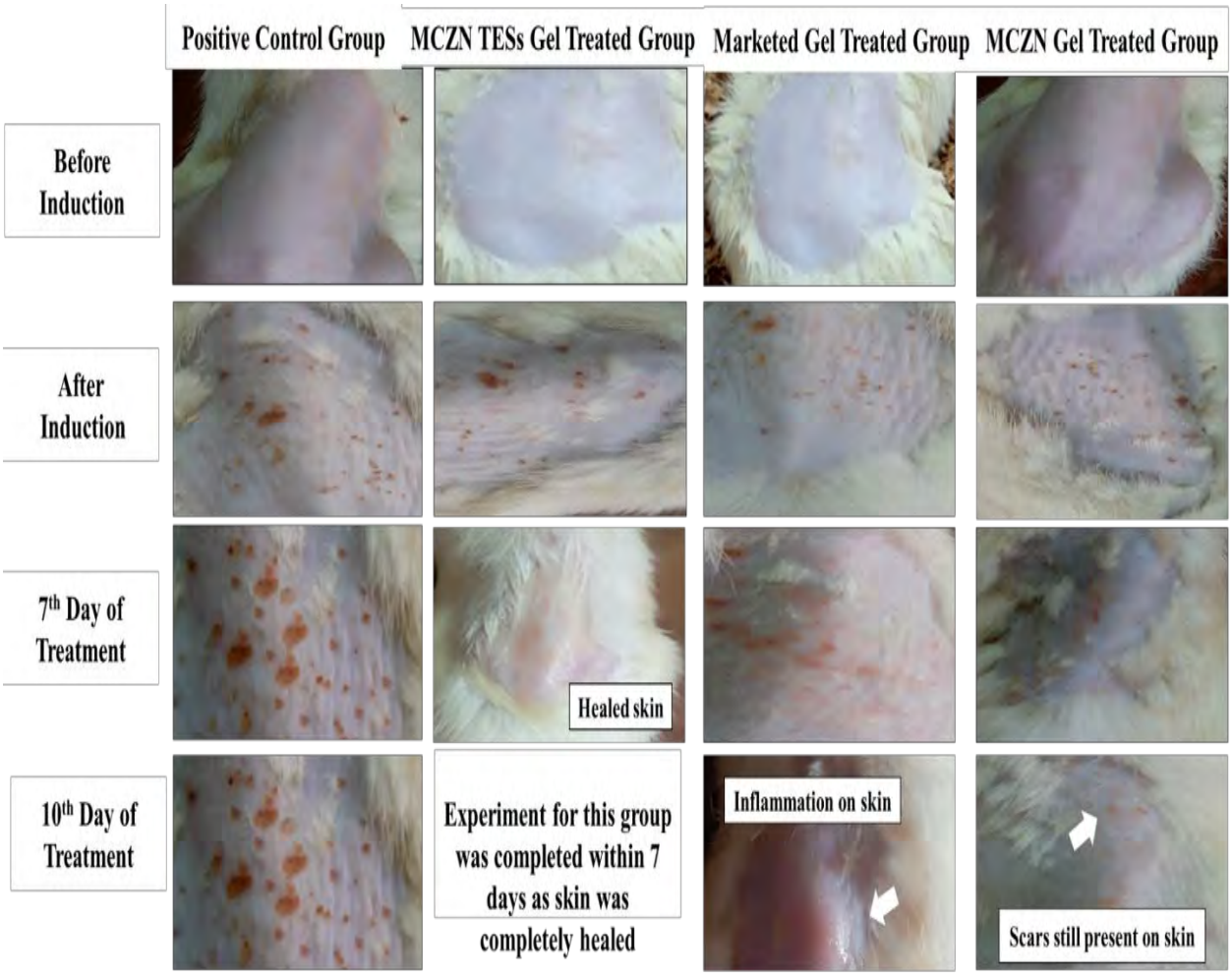

Figure 3.24. Evaluation of rats' skin before and after induction and after treatment.

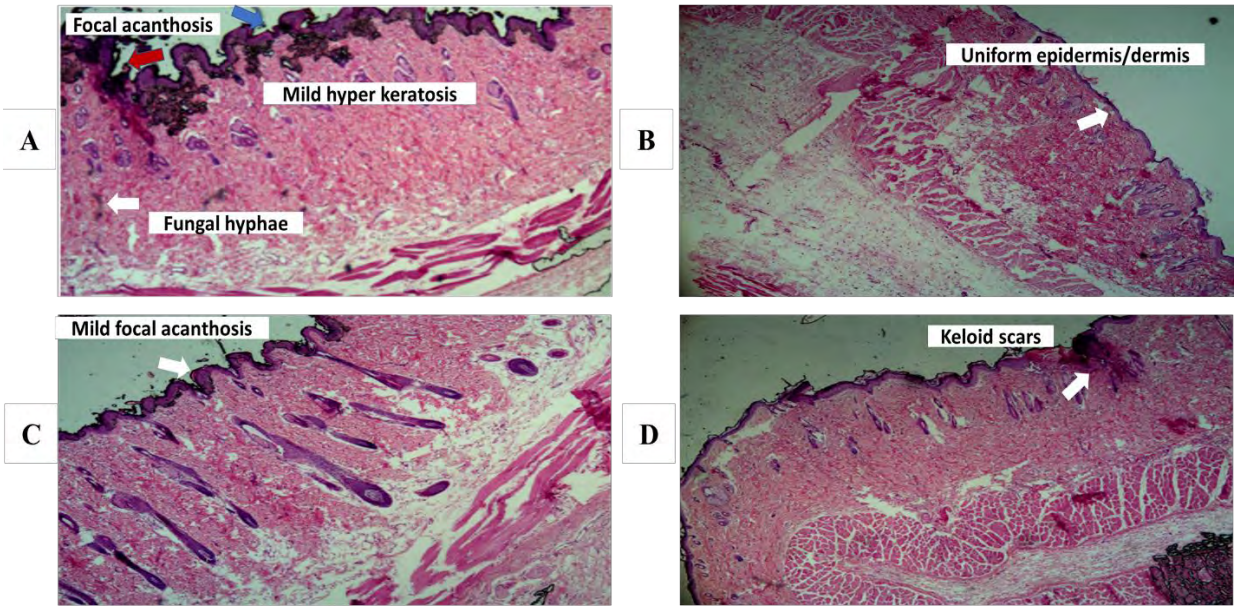

Figure 3.25. Histopathological analysis of rats' skin.
Note: A: *positive control group;* ***B:*** *MCZN TESs Gel treated group;* ***C:*** *Marketed Gel treated group; D MCZN Gel treated group*

Table 3.12. Histopathological examination scoring for quantitative evaluation of antifungal activity.

Groups	Fungal Hyphae	Acanthosis	Hyper keratosis	Keloid scars	Epidermis/ Dermis
Positive Control	1	2	1	0	2
MCZN TESs Gel treated	0	0	0	0	0
Marketed Gel Treated	0	1	0	0	1
MCZN Gel Treated	0	0	0	1	0

Note: Fungal hyphae and Keloid scar: *0 = Absent, 1= Present;* ***Acanthosis, Hyper keratosis:*** *0 = Absent, 1 = Mild, 2 = Severe;* ***Epidermis/ Dermis:*** *0 = Uniform, 1 = Mild inflammation, 2 = Severe inflammation*

3.17: Stability Studies

Stability studies were conducted for MCZN TESs and MCZN TESs Gel for the period of six months**.** In case of MCZN TESs stability data at 25 °C showed increase in PS from 224.81 ± 0.51 nm to 229.81 ± 0.75 nm with PDI increase of 0.207 ± 0.009 to 0.215 ± 0.009, ZP values were decreased from 21.10 ± 1.10 to 19.15 ± 1.15 mV and EE was decreased from 93.12 ± 0.101 to 90.12 ± 0.14% over the period of six months. While at 4 °C changes in MCZN TESs formulation were non-significant as it can be clearly observed from the values given in **Table 3.13**. While for MCZN TESs Gel there was no change in physical appearance of gel and drug content and pH changes were also non-significant ($p < 0.05$) at both 25 °C and 4 °C as shown in **Table 3.14.**

Table 3.13. Stability studies for MCZN TESs.

	0 month		**1 month**		**3 months**		**6 months**	
Temp ° C	**25 °C**	**4 °C**	**25 °C**	**4 °C**	**25 °C**	**4 °C**	**25 °C**	**4 °C**
Physical appearance	Stable, No colour change	Stable, No colour change	Stable, No colour change	Stable, No colour change	Stable, No colour change	Stable, No colour change	Stable, No colour change	Stable, No colour change
Particle size	224.81 ± 0.51	224.81 ± 0.51	227.09 ± 0.65	224.01 ± 0.43	228.8 ± 0.59	225.81 ± 0.92	229.81 ± 0.75	226.8 ± 0.29
Zeta potential	21.10 ± 1.10	21.10 ± 1.10	20.15 ± 0.29	21.02 ± 1.08	20.11 ± 1.19	20.25 ± 1.05	19.15 ± 1.15	20.21 ± 1.1
PDI	0.207 ± 0.009	0.207 ± 0.009	0.209 ± 0.052	0.207 ± 0.009	0.210 ± 0.076	0.207 ± 0.009	0.215 ± 0.009	0.207 ± 0.05
EE (%)	93.12 ± 0.101	93.12 ± 0.101	92.12 ± 0.101	93.10 ± 0.25	91.12 ± 0.101	92.11 ± 0.32	90.12 ± 0.11	92.12 ± 0.14

Note: *All values represented here are expressed as mean ± S.D. (n=3).*

Table 3.14. Stability studies for MCZN TESs.

Time	**Physical appearance of MCZN TESs Gel**						**Drug content%**		**pH**	
	Colour change		**Grittiness**		**Phase separation**					
	25 °C	**4 °C**	**25 °C**	**4 °C**	**25 °C**	**4 °C**	**25 °C**	**4 °C**	**25 °C**	**4 °C**
0 month	No		No		No		98.87 ± 1.03	98.87 ± 1.03	5.70 ± 0.3	5.7 ± 0.3
1 month	No		No		No		98.87 ± 1.03	98.87 ± 1.03	5.70± 0.3	5.7 ± 0.3
3 months	No		No		No		97.23 ± 1.03	97.39 ± 1.03	5.79 ± 0.3	5.75 ± 0.3
6 months	No		No		No		96.81 ± 1.03	97.01 ± 1.03	5.85 ± 0.3	5.8 ± 0.3

Note: *All values represented here are expressed as mean ± S.D. (n=3).*

CHAPTER 4

DISCUSSION

4. DISCUSSION

All age groups are affected by cutaneous candidiasis, which accounts for 1% of outpatient and 7% of inpatient visits to dermatological clinics. Candida could be the key reason for skin illness or could develop because of other skin conditions such as atopic dermatitis, psoriasis, or already present diaper dermatitis. The entire body may be affected, but Intertrigo, cheilitis, and diaper rash are common manifestations (Taudorf *et al.*, 2019). Candidiasis is an opportunistic disease which is mainly caused by *C. albicans* that is common and widely spread strain (Li et al, 2011). Skin is the major route for topical treatment of diseases. But skin barriers are the major obstacles for the transfer of drugs. Only limited number of drugs having desired physiochemical properties can cross the skin barrier making it very difficult for treatment of skin diseases(El Maghraby *et al.*, 2010; Zeb *et al.*, 2019). So TESs are selected for deep skin penetration they are better than other nanovesicles because they have the ability of very high entrapment efficiency and they contain both ethanol and edge activator which provide them fluidity and elasticity (Bajaj *et al.*, 2021).

MCZN is a topical antifungal agent it is most commonly used for treatment of skin fungal infection and despite of its common use the resistance to this drug is very low that is a positive point in era of increasing resistance to drugs (Barasch and Griffin, 2008). It acts by inhibiting ergosterol synthesis (fungistatic effect) and by the production of ROS species (fungicidal effect) that accounts for its less resistance. Another action of MCZN for prevention of fungal infection is the farnesol production in *Candida* that will inhibit the yeast to mycelium transition (Piérard *et al.*, 2012). MCZN has a poor skin penetration problem which makes its use very difficult for the treatment of cutaneous candidiasis (Elmoslemany *et al.*, 2012; Pandit *et al.*, 2014).

MCZN TESs were prepared because nitrate salt of the drug has lipophilic property with partition coefficient of 6.25 which makes its aqueous skin driving concentration very bad (Elmoslemany *et al.*, 2012). But this problem is easily avoided because TESs have the ability to enhance deposition of drug in the deeper skin layers due to the combined advantages of both ethosomes as well as transferosomes in their composition (Song *et al.*, 2012; Abdulbaqi *et al.*, 2018).

Chitosan based MCZN TESs Gel was prepared. Nano vesicles have very efficient compatibility for gels. Because gels provide desired viscosity and efficient bio-

adhesive property to the nano vesicles (Abdulbaqi *et al.*, 2018). In addition to providing regulated drug release chitosan-based hydrogels are hydrophilic, biocompatible, and biodegradable (Ahmadi *et al.*, 2015). Chitosan is a common substance in the realm of subcutaneous administration and implanted treatments because chitosan-based hydrogel drug delivery system releases a therapeutic payload within the body over a prolong period. Chitosan is preferable for hydrogel due to its absence of immunogenicity and inflammation, which have been brought on by many other subcutaneous materials(Bhattarai *et al.*, 2010).

Thin film hydration procedure was opted for the formulation of TESs. First, blank TESs were prepared and optimized. The optimization data of blank TESs gave the idea for the suitable ranges to put in Box- Behnken Design. MCZN TESs optimization was done by using Box-Behnken Design. The independent variables that were selected for optimization were PL90G, MCZN and S 80. There were four dependent variables which were selected for optimization that were PS, ZP, PDI and EE. All 13 formulations were formulated and effect of independent variables on all the dependent variables was also analysed. This analysis was explained via 3D graphs as shown in **Chapter 3 Figure 3.7, 3.8, 3.9 and 3.10.**

Among lipid, surfactant, and drug the most significant effect on PS is because of lipid, then surfactant and then drug. By increasing the concentration of lipid PS is increasing ($p < 0.001$) (Paolino *et al.*, 2005). The reason of increase in PS is due to the formation of multilamellar vesicles (Hosny *et al.*, 2018). Basically when lipids already dissolved in organic solvents are exposed to aqueous environment their solvation decreases and at critical polarity lipids will aggregate to form disc like structure which will grow later on via aggregation of the lipids and a bilayer structure is formulated (Yang *et al.*, 2012). By increasing lipid more rigid structure of lipid bilayer vesicles will be formulated (El-Nabarawi *et al.*, 2013). In case of surfactant ($p = 0.0056$) PS decreases when concentration of surfactant increases. By increasing surfactant conc. because of their surface active ability there is increase in membrane elasticity and its ability to soften the membrane and cause size reduction (Gillet *et al.*, 2011; Maheshwari *et al.*, 2012) Another property of surfactant that affect the PS and cause its reduction is the ability of surfactant to cause reduction of interfacial tension between matrix of lipid and aqueous medium leading to smaller vesicle formation (Thatipamula *et al.*, 2011;

Alomrani *et al.*, 2014). Also specifically focusing on S 80 having low HLB also accounts for smaller PS due to relation between HLB and surface free energy. More hydrophobicity leads to reduction of surface free energy. And it is a general trend with S 80 that because it has low HLB value it cause vesicles size reduction (Chester *et al.*, 2017; Qushawy *et al.*, 2018). In case of drug (p = 0.0257) effect is not as much significant as compared to the other two factors. But general trend that was observed with drug was by increasing its concentration PS was increasing (Hosny *et al.*, 2018; T. A. Ahmed *et al.*, 2021). 3D graphs clearly indicate this trend as explained in **Figure 3.7.**

In case of ZP drug (p = 0.0013) has the most significant effect on ZP as compared to lipid and surfactant. In pre optimization studies when TESs were formulated it can be clearly seen that vesicles had negative charge. During optimization with Box-Behnken Design vesicles had positive charge. The reason of positive charge is MCZN. Because MCZN is an ionic drug, its nitrate ion has positive charge and this positive charge dominates negative charge of lipid and that is why with increasing concentration of drug positive value of zeta potential are increasing (Qushawy *et al.*, 2018). More over the same pattern was observed in already published data of MCZN SLNs in which drug free vesicles showed negative ZP and drug loaded vesicles showed positive ZP (Shah *et al.*, 2017). In case of lipid (p = 0.0531) the ZP was decreasing with increasing concentration. This may be due to the fact that lipid has a net negative charge on it as already reported in published data (Zhao *et al.*, 2015). So, the results showed that this negative charge is being dominated by positive charge of drug and that is why ZP is decreasing. In case of surfactant (p = 0.0047) there is decrease in ZP with its increasing concentration. Because non-ionic surfactant get adsorbed on the surface of the nanovesicles and cause reduction of ZP (Witayaudom and Klinkesorn, 2017). All these trends are clearly explained in 3D graphs in **Figure 3.8.**

PDI value from 0 to 1 is considered acceptable (Danaei *et al.*, 2018). Increase in concentration of lipid (p = 0.0755) has a synergistic effect on PDI and same goes for drug (p = 0.0162). Because when lipids are increased the diffusion in aqueous phase occurs very slowly in other words process of diffusion is delayed and the free lipid will start aggregating with lipid bilayer and cause increase in vesicle size and enhanced PDI (Michelon *et al.*, 2016). With the increase in surfactant (p = 0.0195) PDI is decreasing

this behaviour can be correlated with the decreased PS as explained earlier. All these trends were explained in 3D graph of **Figure 3.9**.

With the increase in concentration of lipid (p = 0.0852) and drug (p = 0.0015) EE was increased. Because PL90G being flexible in nature when increased in concentration provide more space for the drug to accommodate. So more drug get entrapped at high level of lipid because more space is created (Ghadiri *et al.*, 2012; Kumar *et al.*, 2018). And also MCZN is lipophilic in nature so when content of lipid was increased more drug was entrapped due to enhanced solubility of drug (Ansari *et al.*, 2019). In case of surfactant (p = 0.2386) **Figure 3.10** showed antagonistic effect of surfactant on entrapment because increased concentration of surfactants beyond ideal ranges results in micelles formation in membranes of vesicles. And micelles have very poor ability of carrying drugs so EE decreases (Ahad *et al.*, 2017; Chester *et al.*, 2017).

FTIR analysis was performed for PL90G, MCZN, PM and MCZN TESs as shown in **Figure 3.11**. FTIR analyses compares the standard and test spectra to analyse stretching vibrations (which show changes in atom distance) or the bending vibrations of functional groups (including amino, hydroxyl, and carboxyl). The molecular interaction between MCZN and the excipients used in the formulations was assessed by performing FTIR analyses (Umeyor *et al.*, 2021).Any significant change in the drug's absorption bands, the loss of key functional groups, or the emergence of new bands denotes the presence of a molecular interaction. All the peaks were in accordance with published data of MCZN FTIR (Qushawy *et al.*, 2018). PL90G showed major peaks at 2925 cm^{-1} and 2854 cm^{-1} indicating –C-H stretching, a stretching band of ester carbonyl group at was shown via peak at 1737cm^{-1} (Salama *et al.*, 2020). All the major peaks of MCZN as well as PL90G were preserved in PM and final formulation that was MCZN TESs. Results made it clear that any kind of physical interaction among drug and its components was not present.

DSC analysis of PL90G, MCZN and MCZN TESs was performed as shown in **Figure 3.12** . DSC analysis was performed to check solubility of drug and its physical state in which it was present in the final formulation. The DSC analysis clearly showed a large endothermic peak of MCZN at 186.485°C. This temperature is melting temperature of MCZN which is also reported in published data (Bhalekar *et al.*, 2009).This peak show that MCZN was in crystalline form (Umeyor *et al.*, 2021). As it can be observed from

Figure 3.12 that the endothermic peak disappeared in the final formulation labelled as MCZN TESs. The absence of the peak is the indication of change of state of MCZN from crystalline to more soluble amorphous state. So it can be concluded that MCZN state was changed in final formulation this amorphous form indicated high energy and high disorder enhanced solubility (Qushawy *et al.*, 2018).

TESs essential trait of deformability makes it possible for them to pass through narrow junctions with ease, especially in the stratum corneum of the skin for topical drug delivery. Values near 1 represent the particles possess a strong stress dependent ability. Before and after extrusion values were 224.8 ± 5.1 nm and 211 ± 4.9 nm. So, DI was 0.94 and %DI was 94.196%. elasticity was 2.11 ± 0.02, proving that optimized formulation of MCZN TESs was deformable as well as elastic as it was clearly visible from the results (Rabia *et al.*, 2020; Batool *et al.*, 2021).

Chitosan based MCZN TESs Gel was prepared and characterized. Physical appearance of gel was milky white, and gel was homogenous and clear without any particles. pH of gel was 5.7 ± 0.3. As already reported that for topically applied gels pH should be compatible with the skin and usually pH of 5 to 7 is considered acceptable as reported already (Salim *et al.*, 2020). More over pH pf MCZN TESs Gel was in range and was in accordance with the gels that are applied on skin (Borse *et al.*, 2020). Spreadability experiment was performed for MCZN TESs Gel, and its value was 333.712 ± 9.21%. Studies show that this spreadability value is acceptable for topical gel (Qindeel *et al.*, 2019). **Figure 3.15** shows flow behaviour of MCZN TESs Gel. It was observed that by increasing shear rate viscosity was decreasing. This property indicated shear thinning behaviour of gel that is the most important and wanted characteristic of gels that are applied topically. So, gel was following non-Newtonian flow behaviour. Moreover studies also show that this behaviour is desirable for gel applicability on the skin (Salim *et al.*, 2020).

Experiment of *in vitro* release was carried out at pH 5.5 as shown in **Figure 3.16** for MCZN dispersion, MCZN Gel, Marketed Gel, MCZN TESs and MCZN TESs Gel. Within six hours MCZN dispersion gave release of 100% which means that release was very rapid in case of dispersion. Also, MCZN Gel and Marketed Gel gave rapid release 100 percent and 97.5% within 8 hours. But release was slow in case of MCZN TESs after 24 hours they gave release of 88.043% and MCZN Gel release was even slower,

it was 76.1164% indicating slow and prolonged release profile. The prolonged release behaviour of gel was because the drug had to come out from lipid bilayer of TESs and also TESs were released from the chitosan gel matrix that was the reason of slower release of MCZN TESs Gel when compared with MCZN TESs because for gel drug had to cross two phases to reach dissolution medium. From **Table 3.8** it was observed that R^2 value was highest in Krosmeyer- Peppas model with n=0.306 for MCZN TESs showing fickian diffusion which indicates that the MCZN diffusion was due to the potential chemical gradient. In case of MCZN TESs Gel R^2 value was highest in Higuchi model with diffusion exponent value of 0.479 so diffusion was non-fickian , which was desirable release mechanism for gels (Ansari *et al.*, 2019; Paarakh *et al.*, 2019; Farooq *et al.*, 2022).

Figure 3.18 shows the ex vivo skin permeation study that was performed for MCZN different formulation. After 24 hours total amount of drug permeated in case of MCZN TESs, MCZN TESs Gel, Marketed Gel and MCZN Gel was 369.6406 µg/cm^2, 254.1406 µg/cm^2, 77.8210 µg/cm^2 and 73.2112 µg/cm^2 respectively. Permeation was highest in case of MCZN TESs however, Marketed Gel and MCZN Gel showed least permeation because of the poor penetration property of MCZN (Pandit *et al.*, 2014). MCZN TESs had the highest permeation as compared to gels. And MCZN TESs Gel showed much higher permeation as compared to Marketed Gel and MCZN Gel. This highest permeation values for TESs are due to its components. Because ethanol cause fluidization effect, moreover destabilization effect of S 80 cause enhanced permeation for TESs formulations (Garg *et al.*, 2017). From **Figure 3.18** it was observed that for MCZN TESs and MCZN TESs gel during initial hours the release was rapid and then it became sustained because initial rapid release was due to desorption of drug from the vesicles surface afterward there was slow release due to diffusion process followed by drug for release from lipid bilayer (Qushawy *et al.*, 2018). **Table 3.9** showed maximum flux for MCZN TESs i.e., 15.401 with enhancement ratio of 5.049 and flux of MCZN TESs Gel was 10.589 with enhancement ratio of 3.471 much higher as compared to Marketed Gel and MCZN Gel.

Deposition studies were performed which showed that in case of MCZN TESs Gel maximum amount of drug was deposited in epidermis/dermis i.e., 50.87%. In case of MCZN TESs 28% of drug was retained in epidermis/dermis. This showed that transethosomes had the capability of penetrating into deeper layer of skin for local

therapeutic action as compared to Marketed Gel and MCZN Gel in which deposition of drug was only 13.1% and 12.21% respectively as shown in **Figure 3.19**. Hence, it was concluded that MCZN TESs Gel deposition in epidermis/dermis was enhanced 4-folds when compared with Marketed Gel and 4.2-folds when compared with MCZN Gel. The distinctive flexibility of the vesicular membranes in case of TESs, aids in transporting the vesicles through the rough layer of the skin while keeping maximum amount of drug entrapped in the dermal layers, is the reason for maximum deposition of MCZN TESs Gel (Garg *et al.*, 2017).

Skin irritation studies were performed for MCZN TESs Gel and was compared with 0.8% formalin treated skin and untreated skin was kept as control. Scoring was done according to Draize scoring procedure as shown in **Table 3.10.** PDII for formalin treated skin was 3.75 much high as compared to MCZN TESs Gel treated skin where PDII was 1 that showed the good and non-irritant quality of MCZN TESs Gel. **Figure 3.21** shows FTIR analysis of untreated skin and MCZN TESs Gel treated skin. Peaks at 2991 cm^{-1} and 2924 cm^{-1} of normal skin showed that lipid bilayer of skin was not affected it was intact. In case of MCZN TESs Gel treated skin there was a very slight shift in the peaks at this region. Peaks at protein C-N stretching region of normal and treated skin were very slightly different. Difference was almost negligible indicating no change in proteins structure (Mandawgade and Patravale, 2008). Therefore, it was concluded that MCZN TESs Gel crossed the skin without affecting its structure.

Antifungal assay was performed against *C. albicans.* **Figure 3.22** shows black circles indicating ZOI. **Figure 3.23** shows that MCZN TESs gel zone of inhibition was 43 mm much greater as compared to Marketed Gel (Daktarin 2% Gel) and MCZN Gel having ZOI of 20 mm and 18 mm respectively. Maximum ZOI for MCZN TESs Gel was because of maximum sensitivity of this gel against *C. albicans*. These results clearly indicated that antifungal activity of MCZN was significantly enhanced when it was incorporated in TESs, 2.15-folds in comparison to Marketed Gel and 2.38-folds in comparison to MCZN Gel. Because studies show that TESs have better penetrating ability into the cell wall of fungi. So, TESs penetrated and caused retardation of synthesis of ergosterol and resulted in inhibition of growth of fungi (Tabrizi *et al.*, 2017).

In vivo antifungal assay was performed on rats to further confirm the results. Before induction with fungal strains all rats' skins were normal having no signs of infection as shown in **Figure 3.24**. At the 7th day all rats' skin fully showed symptoms of infection that were explained in **Table 3.11**. Rashes/colour changes, cracking, scaling, erythema, and inflammation all these symptoms were present on the skin. Positive control group in which no treatment was given infection got worse with the passage of time as it can be clearly seen in **Figure 3.24**. MCZN TESs Gel treated group was healed completely within 7 days. Before and after treatment observation are explained in **Table 3.11** for MCZN TESs Gel treated group. While in case of Marketed Gel treated group and MCZN Gel treated group took 10 days for healing. At 10th day slight inflammation was present in Marketed Gel treated group and little scars were left in case of MCZN Gel treated group. Duration of treatment for these two groups was 1.5-times extensive than MCZN TESs Gel treated group. Moreover, histological studies were performed. Positive control group in **Figure 3.25: A** showed focal acanthosis marked with red arrow along with mild hyper keratosis marked with blue arrow and with fungal hyphae shown with white arrow clearly proving that infection was increased with the passage of time. **Figure 3.25: B** shows MCZN TESs Gel treated group with uniform epidermis and dermis pointed out with white arrow these results were in alignment with the results visually shown in **Figure 3.24** in which rat skin was completely healed. **Figure 3.25: C** shows Marketed Gel treated group skin was normal but there was mild focal acanthosis as shown with white arrow. **Figure 3.25: D** shows MCZN Gel treated group having keloid scarred skin marked with white arrow. These histopathological studies were in alignment with the observational studies of rats' skin. These results were further supported quantitively using scoring system of histopathological examination as presented in **Table 3.12.** So, it was deduced from *in vivo* model of cutaneous candidiasis that antifungal property of MCZN TESs was clearly and significantly enhanced with better healing quality, brief duration of treatment along with improved histology. This could be due to higher penetration properties of TESs which accounts for their greater accessibility to the deeper skin layer where infection was present. So, MCZN when loaded in TESs can penetrate deeply and get deposited into dermal layers of skin, this localized accumulation of MCZN resulted in early eradication of infection

Stability studies were performed for MCZN TESs for the period of six month at 4 °C and 25 °C. **Table 3.13** shows that change was not significant in PS, PDI, ZP and EE at

4 °C. At 25 °C PS and PDI was increased and ZP, EE was decreased over the period of six month, but changes were not major. So, both temperature for storage of MCZN TESs were suitable. In case of MCZN TESs Gel stability data demonstrated no significant changes in stability of gel over the period of six months. Hence, it was concluded that the prepared gel could be suitably use for efficient topical drug delivery.

CONCLUSIONS

- MCZN loaded TESs were effectively fabricated by thin film hydration method and formulation was successfully optimized and characterized.
- Results indicated formulation had desirable PS with less PDI, good ZP and very efficient EE and there were no interactions between formulation and its excipients and solubility was also enhanced with good deformability and elasticity.
- MCZN TESs were efficiently loaded in chitosan gel and gel characterization showed that gel was clear, uniform and gel had pH desirable for skin application, with good spreadability, desirable viscosity, good drug content and flow behaviour.
- *In vitro* release behaviour of MCZN TESs and MCZN TESs Gel showed prolonged release behaviour and release was diffusion controlled. Ex vivo skin permeation indicated that MCZN TESs and MCZN TESs gel had excellent permeation as compared to Marketed Gel and MCZN Gel and deposition was significantly enhanced in epidermis/dermis. Skin irritation studies showed gel was non-irritant.
- Antifungal assay and *in vivo* studies showed that MCZN TESs Gel antifungal activity was significantly enhanced in comparison to Marketed Gel and MCZN Gel with efficient penetration and shorter duration of treatment.
- It was concluded that MCZN TESs Gel could be effectively used for treatment of cutaneous candidiasis. Further studies are needed to deeply investigate antifungal activity of MCZN TESs Gel and to analyse their suitability for clinical translation.

FUTURE PROSPECTIVES

- The efficacy and safety profile of the new dosage form could be better understood by extrapolating *in vivo* data from variety of animal models.
- For the more advanced targeting of fungus different types of ligands could be attached with TESs.
- MCZN can be loaded in combination with any other antifungal drug in TESs for its enhanced antifungal action.

REFERENCES

REFERENCES

Abdelwahed W, Degobert G, Stainmesse S and Fessi H (2006). Freeze-drying of nanoparticles: Formulation, process and storage considerations. Adv Drug Deliv Rev, 58(15): 1688–1713.

Abdulbaqi I M, Darwis Y, Assi RA and Khan NAK (2018). Transethosomal gels as carriers for the transdermal delivery of colchicine: Statistical optimization, characterization, and ex vivo evaluation. Drug Des Devel Ther, 12: 795–813.

Ahad A, Al Saleh A A, Al Mohizea A M, Al Jenoobi F I, Raish M, Yassin AEB and Alam MA. (2017). Formulation and characterization of novel soft nanovesicles for enhanced transdermal delivery of eprosartan mesylate. Saudi Pharm J, 25(7): 1040–1046.

Ahmadi F, Oveisi Z, Samani M and Amoozgar Z. (2015). Chitosan based hydrogels: Characteristics and pharmaceutical applications. Res Pharm Sci, 10(1): 1–16.

Ahmed MM, Fatima F, Anwer MK, Ibnouf EO, Kalam MA, Alshamsan A, Aldawsari MF, Alalaiwe A and Ansari MJ (2021). Formulation and in vitro evaluation of topical nanosponge-based gel containing butenafine for the treatment of fungal skin infection. Saudi Pharm J, 29(5): 467–477.

Ahmed S, Kassem MA and Sayed S (2020). Bilosomes as promising nanovesicular carriers for improved transdermal delivery: Construction, in vitro optimization, ex vivo permeation and in vivo evaluation. Int J Nanomedicine, 15: 9783–9798.

Ahmed TA, Alzahrani MM, Sirwi A and Alhakamy NA (2021). The antifungal and ocular permeation of ketoconazole from ophthalmic formulations containing trans-ethosomes nanoparticles. Pharmaceutics, 13(2): 1–24.

Alam MS, Garg A, Pottoo FH, Saifullah MK, Abu-Izneid T, Manzoor O, Mohsin M and Javed MN (2017). Gum ghatti mediated, one pot green synthesis of optimized gold nanoparticles: Investigation of process-variables impact using Box-Behnken based statistical design. Int J Biol Macromol, 104: 758–767.

Alomrani AH, Shazly GA, Amara AAAF and Badran MM (2014). Itraconazole-hydroxypropyl-β-cyclodextrin loaded deformable liposomes: In vitro skin penetration studies and antifungal efficacy using Candida albicans as model. Colloids Surf, B 121: 74–81.

Alsarra IA (2009). Chitosan topical gel formulation in the management of burn wounds.

Int J Biol Macromol, 45(1): 16–21.

Andrade LM, De Fátima Reis C, Maione Silva L, Anjos JLV, Alonso A, Serpa RC, Marreto RN, Lima EM and Taveira SF (2014). Impact of lipid dynamic behavior on physical stability, in vitro release and skin permeation of genistein-loaded lipid nanoparticles. Eur J Pharm Biopharm, 88(1): 40–47.

Ansari MD, Ahmed S, Imam SS, Khan I, Singhal S, Sharma M and Sultana Y (2019). CCD based development and characterization of nano-transethosome to augment the antidepressant effect of agomelatine on Swiss albino mice. J Drug Deliv Sci Technol, 54(June): 101234.

Bajaj KJ, Parab BS and Shidhaye SS (2021). Nano-transethosomes: A novel tool for drug delivery through skin. Indian J Pharm, 55(1): s1–s10.

Barasch A and Griffin AV(2008). Miconazole revisited: New evidence of antifungal efficacy from laboratory and clinical trials. Future Microbiol, 3(3): 265–269.

Batool S, Zahid F, Ud-Din F, Naz SS, Dar MJ, Khan MW, Zeb A and Khan GM (2021). Macrophage targeting with the novel carbopol-based miltefosine-loaded transfersomal gel for the treatment of cutaneous leishmaniasis: in vitro and in vivo analyses. Drug Dev Ind Pharm, 47(3): 440–453.

De Bernardis F, Mühlschlegel FA, Cassone A and Fonzi WA (1998). The pH of the host niche controls gene expression in and virulence of Candida albicans. Infect Immun, 66(7): 3317–3325.

Bhalekar MR, Pokharkar V, Madgulkar A Patil, Nilam and Patil Nilkanth (2009). Preparation and evaluation of miconazole nitrate-loaded solid lipid nanoparticles for topical delivery. AAPS PharmSciTech, 10(1): 289–296.

Bhattarai N, Gunn J and Zhang M (2010). Chitosan-based hydrogels for controlled, localized drug delivery. Adv Drug Deliv Rev, 62(1): 83–99.

Borse VA, Gangude AB and Deore AB (2020). Formulation and evaluation of antibacterial topical gel of doxycycline hyclate, neem oil and tea tree oil. Indian J Pharm, 54(1): 206–212.

Castro GA, Oliveira CA, Mahecha GAB and Ferreira LAM (2011). Comedolytic effect and reduced skin irritation of a new formulation of all-trans retinoic acid-loaded solid lipid nanoparticles for topical treatment of acne. Arch Dermatol Res, 303(7): 513–520.

Cavrini V, Di Pietra AM and Gatti R (1989). Analysis of miconazole and econazole in pharmaceutical formulations by derivative UV spectroscopy and liquid chromatography (HPLC). J Pharm Biomed, 7(12): 1535–1543.

Chester K, Zahiruddin S, Ahmad A, Khan W, Paliwal S and Ahmad S (2017). Bioautography-based Identification of Antioxidant Metabolites of Solanum nigrum L. and Exploration Its Hepatoprotective Potential agChester, K. et al. (2017). Bioautography-based Identification of Antioxidant Metabolites of Solanum nigrum L. and Explorati. Pharmacogno Mag, 13 (Suppl(62): 179–188.

Conti HR, Huppler AR, Whibley N and Gaffen SL (2014). Animal models for candidiasis. Curr Protoc Immunol, (SUPPL.105): 1–17.

Danaei M, Dehghankhold M, Ataei S, Hasanzadeh Davarani F, Javanmard R, Dokhani A, Khorasani S and Mozafari MR (2018). Impact of particle size and polydispersity index on the clinical applications of lipidic nanocarrier systems. Pharmaceutics, 10(2): 1–17.

El Nabarawi MA, Bendas ER, El Rehem RTA and Abary MYS (2013). Transdermal drug delivery of paroxetine through lipid-vesicular formulation to augment its bioavailability. Int J Pharm, 443(1–2): 307–317.

Elmoslemany RM, Abdallah OY, ElCKhordagui LK and Khalafallah NM (2012). Propylene glycol liposomes as a topical delivery system for miconazole nitrate: Comparison with conventional liposomes. AAPS PharmSciTech, 13(2): 723–731.

Farooq M, Usman F, Zaib S, Shah HS, Jamil QA, Akbar Sheikh F, Khan A, Rabea S, Hagras SAA, El Saber Batiha G and Khan I (2022). Fabrication and Evaluation of Voriconazole Loaded Transethosomal Gel for Enhanced Antifungal and Antileishmanial Activity. Molecules, 27(10): 3347.

Fothergill, AW (2006). Miconazole : a historical perspective.171–175.

Garg V, Singh H, Bhatia A, Raza K, Singh SK, Singh B and Beg S (2017). Systematic Development of Transethosomal Gel System of Piroxicam: Formulation Optimization, In Vitro Evaluation, and Ex Vivo Assessment. AAPS PharmSciTech, 18(1): 58–71.

Ghadiri M, Fatemi S, Vatanara A, Doroud D, Najafabadi AR, Darabi M and Rahimi AA (2012). Loading hydrophilic drug in solid lipid media as nanoparticles: Statistical modeling of entrapment efficiency and particle size. Int J Pharm, 424(1–2): 128–137.

Gillet A, Lecomte F, Hubert P, Ducat E, Evrard B and Piel G (2011). Skin penetration behaviour of liposomes as a function of their composition. Eur J Pharm. Biopharm, 79(1): 43–53.

Haq A and Michniak-Kohn B (2018). Effects of solvents and penetration enhancers on transdermal delivery of thymoquinone: Permeability and skin deposition study. Drug Deliv, 25(1): 1943.

Havlickova B, Czaika VA and Friedrich M (2009). Epidemiological trends in skin mycoses worldwide (Mycoses (2008) 51, SUPPL. 4, (2-15)). Mycoses, 52(1): 95.

Hay R (2013). Superficial fungal infections. CHIN MED UK, 41(12), pp. 716–718.

Hay RJ (1999). The management of superficial candidiasis. J Am Acad Dermatol, 40(6 II): 35–42.

Hosny KM, Ahmed OAA, Fahmy UA and Alkhalidi HM (2018). Nanovesicular systems loaded with a recently approved second generation type-5 phospodiesterase inhibitor (avanafil): I. Plackett-Burman screening and characterization. J Drug Deliv Sci and Technol, 43(September 2017): 154–159.

Kobayashi D, Kondo K, Uehara N, Otokozawa S, Tsuji N, Yagihashi A and Watanabe N (2002). Endogenous reactive oxygen species is an important mediator of miconazole antifungal effect. Antimicrob Agents Chemother, 46(10): 3113–3117.

Kumar JR (2018). Anticandidal activity of ethosomal gel containing miconazole nitrate in male sprague dawley rat. J Pharm Sci, 10(12): 3400–3405.

Kumar L, Verma S, Singh K, Prasad DN and Jain AK (2016). Ethanol Based Vesicular Carriers in Transdermal Drug Delivery: Nanoethosomes and Transethosomes in Focus. NanoWorld Journal, 2(3): 41–51.

Kumar P, Singh S, Handa V and Kathuria H (2018). Oleic Acid Nanovesicles of Minoxidil for Enhanced Follicular Delivery. Medicines, 5(3): 103.

Li et al (2011). © Chinese Medical Association Publishing House Downloaded from med Central.net on [February 24, 2022]. For personal use only medical Association publishing house, 35–44.

El Maghraby GMM, Williams AC and Barry BW (2010). Skin hydration and possible shunt route penetration in controlled estradiol delivery from ultradeformable and standard liposomes. J Pharm Pharmacol, 53(10): 1311–1322.

Maheshwari RGS, Tekade RK, Sharma PA, Darwhekar G, Tyagi A, Patel RP and Jain DK (2012). Ethosomes and ultradeformable liposomes for transdermal delivery of clotrimazole: A comparative assessment. Saudi Pharm J, 20(2): 161–170.

Mandawgade SD and Patravale VB (2008). Development of SLNs from natural lipids: Application to topical delivery of tretinoin. Int J Pharm, 363(1–2): 132–138.

Martins N, Ferreira ICFR, Barros L, Silva S and Henriques M (2014). Candidiasis: Predisposing Factors, Prevention, Diagnosis and Alternative Treatment. Mycopathologia, 177(5–6): 223–240.

Mathur M and Devi VK (2017). Potential of novel drug delivery systems in the management of topical candidiasis. J Drug Target, 25(8): 685–703.

Michelon M, Mantovani RA, Sinigaglia Coimbra R, de la Torre LG and Cunha RL (2016). Structural characterization of β-carotene-incorporated nanovesicles produced with non-purified phospholipids. Int. Food Res J, 79: 95–105.

Mohamed Firthouse PU, Mohamed Halith S, Wahab SU, Sirajudeen M and Kadher Mohideen S (2011). Formulation and evaluation of Miconazole niosomes. Int J Pharmtech Res, 3(2): 1019–1022.

Mohammed BS and Al Gawhari FJ (2021). Transethosomes a novel transdermal drug delivery system for antifungal drugs. Int J Drug Deliv Technol , 11(1): 238–243.

Nawanopparatsakul S (2005). Skin irritation test of curcuminoids facial mask containing chitosan as a binder. … Uni versity J, 140–147.

Ni X and Streett DA (2005). Modulation of water activity on fungicide effect on Aspergillus niger growth in Sabouraud dextrose agar medium. Lett Appl Microbiol. 41(5): 428–433.

Nurahmanto D (2013). Development and validation of UV spectrophotometric method for quantitative estimation of Promethazine HCl in phosphate buffer saline pH 7.4. Intt Curr Pharm J, 2(8): 141–142.

Nurhan AD (2010). Dash, Murthy',Polish Pharmaceutical Society, 67(3): 217–223.

Odds FC (1994). Pathogenesis of Candida infections. J Am Acad Dermatol, 31(3): S2–S5.

Paarakh MP, Jose PANI, Setty CM and Peter GV (2019). Release Kinetics – Concepts and Applications. International Journal of Pharmacy Research & Technology, 8(1): 12–

20.

Pandit J, Garg M and Jain NK (2014). Miconazole nitrate bearing ultraflexible liposomes for the treatment of fungal infection. J Liposome Res, 24(2): 163–169.

Paolino D, Lucania G, Mardente D, Alhaique F and Fresta M (2005). Ethosomes for skin delivery of ammonium glycyrrhizinate: In vitro percutaneous permeation through human skin and in vivo anti-inflammatory activity on human volunteers. JCR, 106(1–2): 99–110.

Piérard GE, HermannsLê T, Delvenne P and Piérard Franchimont C (2012). Miconazole, a pharmacological barrier to skin fungal infections. Expert Opin Pharmacother, 13(8): 1187–1194.

Qindeel M, Ahmed N, Sabir F, Khan S and Ur Rehman A (2019). Development of novel pH-sensitive nanoparticles loaded hydrogel for transdermal drug delivery. Drug Dev Ind Pharm, 45(4): 629–641.

Qushawy M, Nasr A, Abd Alhaseeb M and Swidan S (2018). Design, optimization and characterization of a transfersomal gel using miconazole nitrate for the treatment of candida skin infections. Pharmaceutics, 10(1).

Rabia S, Khaleeq N, Batool S, Dar MJ, Kim DW, Din FU and Khan GM (2020). Rifampicin-loaded nanotransferosomal gel for treatment of cutaneous leishmaniasis: Passive targeting via topical route. Nanomed J, 15(2): 183–203.

Rachmawati H, Edityaningrum CA and Mauludin R (2013). Molecular inclusion complex of curcumin-β-cyclodextrin nanoparticle to enhance Curcumin skin permeability from hydrophilic matrix gel. AAPS PharmSciTech, 14(4): 1303–1312.

Ruhnke M (2006). Epidemiology of Candida albicans Infections and Role of Non-Candidaalbicans Yeasts. Curr Drug Targets, 7(4): 495–504.

Salama A, Badran M, Elmowafy M and Soliman GM (2020). Spironolactone-loaded leciplexes as potential topical delivery systems for female acne: In vitro appraisal and ex vivo skin permeability studies. Pharmaceutics, 12(1): 1–17.

Salim MW, Shabbir K, ud-Din F, Yousaf AM, Choi HG and Khan GM (2020). Preparation, in-vitro and in-vivo evaluation of Rifampicin and Vancomycin Co-loaded transfersomal gel for the treatment of cutaneous leishmaniasis. J Drug Deliv Sci Technol, 60(May): 101996.

Shah RM, Eldridge DS, Palombo EA and Harding IH (2017). Microwave-assisted microemulsion technique for production of miconazole nitrate- and econazole nitrate-loaded solid lipid nanoparticles. Eur J Pharm Biopharm, 117: 141–150.

Shokry M, Hathout RM and Mansour S (2018). Exploring gelatin nanoparticles as novel nanocarriers for Timolol Maleate: Augmented in-vivo efficacy and safe histological profile. Int J Pharm. 545(1–2): 229–239.

Simõe, andreia ascenso, sara raposo, cátia B, cardoso TMF, garcia PMV, lopes BBS (2015). IJN-86186-development--characterization-and-skin-delivery-studies-of-r. Int J Nanomedicine, 10: 5837–5851.

Song CK, Balakrishnan P, Shim CK, Chung SJ, Chong S and Kim DD (2012). A novel vesicular carrier, transethosome, for enhanced skin delivery of voriconazole: Characterization and in vitro/in vivo evaluation. Colloids Surf B, 92: 299–304.

Sriram G, Teja KV and Vasundhara KA (2019). Antimicrobial efficacy of novel ethanolic extract of morinda citrifolia against enterococcus faecalis by agar well diffusion and broth dilution methods - An invitro study. Braz Dent Sci, 22(3): 365–370.

Tabrizi MM, Hosseini SA and Akbarzadeh A (2017). Liposome & Nanotechnology Book (September 2019).

Tasneem U, Siddiqui MT, Faryal R and Shah AA (2017). Prevalence and antifungal susceptibility of Candida species in a tertiary care hospital in Islamabad, Pakistan. JPMA, 67(7): 986–991.

Taudorf EH, Jemec GBE, Hay RJ and Saunte DML (2019). Cutaneous candidiasis – an evidence-based review of topical and systemic treatments to inform clinical practice. J Eur Acad Dermatol Venereol, 33(10): 1863–1873.

Thatipamula RP, Palem CR, Gannu R, Mudragada S and Yamsani MR (2011). Formulation and in vitro characterization of domperidone loaded solid lipid nanoparticles and nanostructured lipid carriers. DARU, J Pharm Sci, 19(1): 23–32.

Umeyor CE, Okoye I, Uronnachi E, Okeke T, Kenechukwu F and Attama A (2021). Repositioning miconazole nitrate for malaria: Formulation of sustained release nanostructured lipid carriers, structure characterization and in vivo antimalarial evaluation. J Drug Deliv Sci Technol, 61(May 2020): 102125.

Wavikar P and Vavia P (2013). Nanolipidgel for enhanced skin deposition and improved antifungal activity. AAPS PharmSciTech, 14(1): 222–233.

Witayaudom P and Klinkesorn U (2017). Effect of surfactant concentration and solidification temperature on the characteristics and stability of nanostructured lipid carrier (NLC) prepared from rambutan (Nephelium lappaceum L.) kernel fat. J Colloid Interface Sci, 505: 1082–1092.

Yang K, Delaney JT, Schubert US and Fahr A (2012). Fast high-throughput screening of temoporfin-loaded liposomal formulations prepared by ethanol injection method. J Liposome Res, 22(1): 31–41.

Zeb A, Arif ST, Malik M, Shah FA, Din FU, Qureshi OS, Lee ES, Lee GY and Kim JK (2019). Potential of nanoparticulate carriers for improved drug delivery via skin. J Pharm Investig, 49(5): 485-517.

Zhao L, Temelli F, Curtis JM and Chen L (2015). Preparation of liposomes using supercritical carbon dioxide technology: Effects of phospholipids and sterols. Int Food Res J, 77 63–72.

Miconazole Nitrate loaded transethosomes_Maryam

ORIGINALITY REPORT

6%	3%	4%	2%
SIMILARITY INDEX	INTERNET SOURCES	PUBLICATIONS	STUDENT PAPERS

PRIMARY SOURCES

1	Submitted to University of Birmingham Student Paper	1%
2	Submitted to Higher Education Commission Pakistan Student Paper	<1%
3	Mahima Mathur, V. Kusum Devi. " Potential of novel drug delivery systems in the management of topical ", Journal of Drug Targeting, 2017 Publication	<1%
4	Rishabha Malviya, Rajendra Awasthi, Pramod Kumar Sharma, Susheel Kumar Dubey. " Stabilization of Etoricoxib Nanosuspension Using Gum and Copolymers: Preparation, Characterization, and Cytotoxic Study ", ASSAY and Drug Development Technologies, 2021 Publication	<1%
5	Kashaf Bashir, Muhammad Farhan Ali Khan, Aiyeshah Alhodaib, Naveed Ahmed et al. "Design and Evaluation of pH-Sensitive	<1%